Molecular Therapy
Methods & Clinical Development
Original Article

Lentiviral delivered aflibercept OXB-203 for treatment of neovascular AMD

Sharifah Iqball,[1] Daniel K. Beck,[1,2] Gayathri Devarajan,[1,2] Cheen P. Khoo,[1,2] Deirdre M. O'Connor,[1] Scott Ellis,[1] Efrain Guzman,[1] Kyriacos A. Mitrophanous,[1] and Yatish Lad[1]

[1]Oxford Biomedica (UK) Ltd., Windrush Court, Transport Way, OX4 6LT Oxford, UK

Neovascular age-related macular degeneration (nAMD) is a leading cause of blindness in the aging population, with vascular endothelial growth factor (VEGF) playing a key role. Treatment with recombinant anti-VEGFs is the current standard of care; however, it is only effective for 1–2 months at a time and requires re-administration. Gene therapy could pave the way for stable, long-term expression of therapeutic anti-VEGF with a single dose, reducing the frequency of treatment and potentially improving clinical outcomes. As such, we have developed OXB-203, a lentiviral-based gene therapy encoding the anti-VEGF protein aflibercept. Aflibercept derived from OXB-203 exhibited comparable *in vitro* binding characteristics to VEGF as recombinant aflibercept. Furthermore, its biological potency was demonstrated by the equivalent inhibition of VEGF-induced human umbilical vein endothelial cell (HUVEC) proliferation and tubule formation as recombinant aflibercept. In a rat choroidal neovascularization (CNV) model of nAMD, a single subretinal administration of OXB-203 reduced laser-induced CNV lesion areas analogous to an intravitreal bolus of recombinant aflibercept. Finally, in a head-to-head comparative study, aflibercept derived from OXB-203 was shown to be expressed at significantly higher levels in ocular tissues than from an AAV8-aflibercept vector following a single subretinal delivery to rats. These findings support the therapeutic potential of OXB-203 for the management of nAMD.

INTRODUCTION

Age-related macular degeneration (AMD) has emerged to be the most common cause of vision impairment in the elderly population,[1,2] characterized by degeneration of the macula and resulting in blurred or distorted areas in the central visual field.[3] Neovascular AMD (nAMD) develops as a result of the growth of abnormal blood vessels, emanating from the choroidal circulation or from the retinal vasculature.[4] This choroidal neovascularization (CNV) results in the exudative or "wet" form of AMD, which is depicted by the leakage of blood and fluid from the aberrant neovasculature into the retina. Accumulation of fluid within the retina leads to photoreceptor degeneration, secondary fibrosis, and atrophy.[3,4] It has been demonstrated that overexpression of vascular endothelial growth factor A (VEGFA) is a major driver of the generation and progression of nAMD. As such, VEGFA has become the primary target for developing treatments, and three recombinant anti-VEGFA therapies, ranibizumab,[5] bevacizumab,[6] and aflibercept,[7] have become the standard of care. Although anti-VEGFA therapies have been successful in the clinic, a major disadvantage for their practical use is the need for repeated intravitreal (IVT) injections at regular intervals, every 4–8 weeks[8] depending on the therapy, disease progression, and patient compliance. This regimen involves frequent visits to healthcare providers, injection discomfort, sustained intraocular pressure, and increased risk of infection and cataracts;[9–12] and as a result, long-term follow-up studies of anti-VEGFA treatments have shown that patient compliance is reduced to less than 50%,[9,13,14] leading to disease progression and vision loss.[9,15]

The development of new agents for nAMD has focused on both improving the efficacy and extending the duration of action. An anti-VEGFA drug, brolucizumab, approved by the U.S. Food and Drug Administration (FDA) in 2019, has the potential to extend the dosing regimen to every 12 weeks,[16] reducing the treatment burden compared with the current standard of care. A higher dose of aflibercept is being trialed (Phase 3, PULSAR study; ClinicalTrials.gov: NCT04423718; Bayer)[17] that could potentially extend the current dosing regimen from 8 weeks to 12–16 weeks with this higher dose. Long-acting drug delivery (LAD) systems that can provide sustained drug exposure from a single administration could mitigate the problems associated with frequent IVT injections.[18,19] Several strategies are actively being investigated, most of which are in pre-clinical or clinical development. These include slow-release formulations (e.g., encapsulation of the anti-VEGFs in a thermogel depot for sustained delivery),[20] continuous delivery drug devices such as Roche's Port Delivery System (PDS) with ranibizumab, currently in a Phase 3 clinical trial,[21] as well as gene therapies with viral vectors. Lentiviral vectors expressing pigment epithelium-derived factor (PEDF)[22] or a single-chain antibody directed against VEGF (scFv V65)[23] or multigenic lentiviral vectors encoding anti-angiogenic microRNAs[24] have been shown to be effective in treating laser-induced CNV in rodent models

Received 27 October 2022; accepted 12 July 2023;
https://doi.org/10.1016/j.omtm.2023.07.001.

[2]These authors contributed equally

Correspondence: Sharifah Iqball, Oxford Biomedica (UK) Ltd., Windrush Court, Transport Way, OX4 6LT Oxford, UK.
E-mail: s.iqball@oxb.com

of nAMD. Clinical trials are currently ongoing for gene therapy with adeno-associated viral vectors (AAV) encoding either aflibercept[25–27] (Phase 1, OPTIC study [ClinicalTrials.gov: NCT03748784]; OPTIC-EXT [ClinicalTrials.gov: NCT04645212]; and more recently, Phase 2, LUNA study [Clinical Trials.gov: NCT05536973] with IVT delivery of ADVM-022 [Ixo-vec, Adverum Biotechnologies])[28,29] or an anti-VEGFfab similar to ranibizumab[30,31] (Phase 2/3, ATMOSPHERE study [ClinicalTrials.gov: NCT04704921]and Phase 3, ASCENT study [ClinicalTrials.gov: NCT05407636] with subretinal delivery of RGX-314; Phase 2, AAVIATE study [ClinicalTrials.gov: NCT 04514653] with suprachoroidal delivery of RGX-314 [Regenxbio]).[32,33] These therapies have the potential to improve upon the current standard of care, enabling long-term sustained expression of the vector-derived therapeutic anti-VEGF protein from the retina, with the use of a single dose.

RetinoStat®, a lentiviral-based gene therapy and predecessor of OXB-203 for the treatment of nAMD, expressing endostatin and angiostatin, has been shown to suppress CNV lesions and reduce associated blood vessel leakage with a single subretinal dose of the vector in a mouse model of nAMD.[34,35] In the 21-patient Phase I GEM study[36] (ClinicalTrials.gov: NCT01301443) and follow-up study (ClinicalTrials.gov: NCT01678872), RetinoStat® demonstrated stable and long-term expression of both proteins in the aqueous humor of patients out to 6 years following a single subretinal dose, providing proof of principle for this type of single-dose gene therapy approach. OXB-203 carries the coding sequence of the anti-VEGF protein, aflibercept, which is a human recombinant fusion protein comprising the second immunoglobulin (Ig) domain of human VEGF receptor 1 (VEGFR1) and the third Ig domain of human VEGFR2, which are fused to the constant region (Fc [fragment crystallizable region]) of human IgG1.[37] It acts as a soluble decoy receptor and binds to VEGFA, VEGFB, and placental growth factor (PlGF) and inhibits activation of VEGF receptors and proliferation of endothelial cells, thereby reducing the growth of new blood vessels under the macula and slowing the progression of nAMD.[38] Whereas RetinoStat® is based solely on the equine infectious anemia virus (EIAV) platform, OXB-203 has been evaluated with the EIAV (OXB-203E) and human immunodeficiency virus (HIV-1, OXB-203H) lentiviral vector platforms. In the current study, we investigated the *in vitro* functional characteristics of OXB-203 vector-derived aflibercept alongside recombinant aflibercept. The *in vivo* efficacy of a single subretinal administration of OXB-203E to a rat model of nAMD was compared to the standard of care, an IVT bolus of recombinant aflibercept. Vector-derived aflibercept expression from OXB-203E, OXB-203H, and AAV8-aflibercept (AAV8-aflib, encoding the same transgene and driven by the same promoter as OXB-203) was evaluated *in vivo* following a single subretinal administration in order to compare the aflibercept productivity from the lentiviral vectors to that from an AAV vector currently being trialed in gene therapies for nAMD. The vector doses for this study were based on the allometrically scaled clinical doses for a subretinally administered lentiviral vector and an AAV for nAMD.

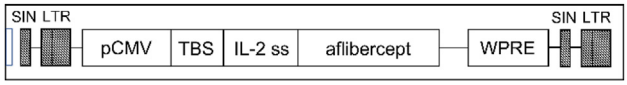

Figure 1. Construction of a lentiviral vector expressing aflibercept
Schematic representation of the vector genome encoding codon-optimized aflibercept. SIN, self-inactivating vector; LTR, long terminal repeat; pCMV, human cytomegalovirus promoter, TBS, tryptophan RNA-binding attenuation protein (TRAP) binding sequence; IL-2 ss, IL-2 secretory signal sequence; WPRE, woodchuck hepatitis virus post-transcriptional regulatory element.

RESULTS

Characterization of lentiviral vector-derived aflibercept protein

OXB-203E and OXB-203H encode the same aflibercept transgene cassette (Figure 1). The biochemical and functional properties of OXB-203 vector-derived aflibercept protein were compared to that of recombinant aflibercept. Expression of aflibercept was first evaluated in HEK293T cells transduced at matched multiplicity of infection (MOI) of OXB-203E and OXB-203H. The titer for the concentrated vector of OXB-203H (2.5×10^8 transducing units [TU]/mL) was 2.3-fold higher compared to OXB-203E (1.1×10^8 TU/mL) when produced using adherent HEK293T cells and 7.7-fold higher for OXB-203H (6.1×10^9 TU/mL) compared to OXB-203E (7.9×10^8 TU/mL) when produced using suspension HEK293T cells. OXB-203H vector-derived aflibercept expression, when normalized to vector copy number (VCN) from transduced HEK293T cells, was significantly higher by 1.4- to 2.1-fold ($p \leq 0.01$) compared to that from OXB-203E transduced cells at each matched MOI tested (Figure 2A). Transduction of HEK293T with OXB-Null (EIAV-Null) or HIV-Null did not result in any measurable expression of aflibercept (data not shown). Western blot analysis of OXB-203 vector-derived aflibercept and recombinant aflibercept were of the expected molecular weight of ~70 kDa from all sources (Figure 2B); an additional unreported protein product of higher molecular weight than expected was observed for recombinant aflibercept.

As OXB-203E and OXB-203H encode the same transgene cassette, it is expected that the aflibercept protein produced from cells transduced by these vectors would have the same protein characteristics. To confirm this, binding affinity was assessed between recombinant human $VEGFA_{165}$ ($rhVEGFA_{165}$) and OXB-203 vector-derived aflibercept using a cell-free assay. Depletion of the unbound $rhVEGFA_{165}$ was detected by addition of increasing quantities of either OXB-203 vector-derived aflibercept or recombinant aflibercept (Figure 2C). The binding affinity profiles and IC_{50} values for OXB-203E and OXB-203H vector-derived aflibercept were comparable ($p > 0.99$) to those of recombinant aflibercept. However, approximately 1.4 pM of detectable $rhVEGFA_{165}$ remained unbound in all samples despite a 10-fold increase in the aflibercept concentration, as reported previously.[39,40] A saturation binding assay used to determine the binding kinetics of $rhVEGFA_{165}$ to OXB-203E or OXB-203H vector-derived aflibercept or to recombinant aflibercept showed no significant differences in the calculated maximum specific binding

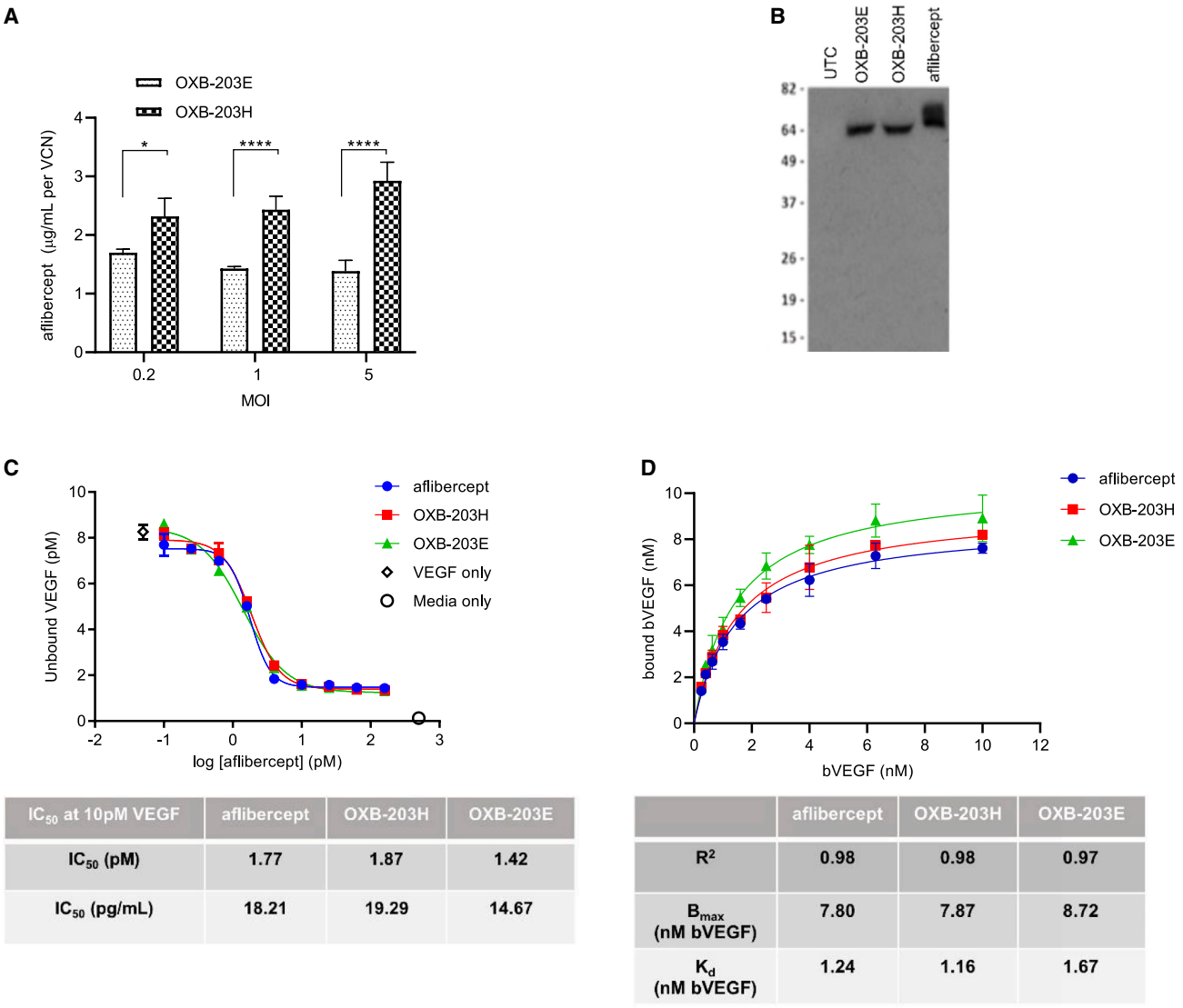

IC_{50} at 10pM VEGF	aflibercept	OXB-203H	OXB-203E
IC_{50} (pM)	1.77	1.87	1.42
IC_{50} (pg/mL)	18.21	19.29	14.67

	aflibercept	OXB-203H	OXB-203E
R^2	0.98	0.98	0.97
B_{max} (nM bVEGF)	7.80	7.87	8.72
K_d (nM bVEGF)	1.24	1.16	1.67

Figure 2. Biochemical characterization of OXB-203 vector-derived aflibercept

(A) Quantification of OXB-203 vector-derived aflibercept in supernatants from MOI-matched, vector transduced HEK293T cells, normalized to vector copy number (VCN). Bars represent means of duplicate transductions (n = 1). An asterisk denotes significance. (B) Western blot of 7.5 ng OXB-203 vector-derived and recombinant aflibercept under reducing conditions (n = 1). UTC: supernatant from untransduced HEK293T. (C) Binding affinities of OXB-203 vector-derived aflibercept to rhVEGFA$_{165}$ (n = 1). (D) Saturation binding curve with OXB-203 vector-derived or recombinant aflibercept and titration to biotinylated rhVEGFA$_{165}$ (bVEGF) (n = 1). Maximum specific binding (B_{max}) and the dissociation constant (K_d) were calculated for bVEGF to aflibercept. Error bars in all figures indicate SD for duplicate samples.

(B_{max}) or the dissociation constant (K_d) (Figure 2D) for all three aflibercept proteins.

The biological potency of OXB-203E vector-derived aflibercept was assessed in a VEGF-induced human umbilical vein endothelial cell (HUVEC) proliferation and Matrigel tubule formation assays. OXB-203E vector-derived aflibercept inhibited HUVEC proliferation by 38.3% relative to the control supernatant (Figure 3A). This inhibition was comparable to that observed with the same concentration of recombinant aflibercept at 34.6%[41] and was significantly higher ($p < 0.0001$) than that from the supernatant of OXB-Null transduced cells. Cell proliferation was unaffected by an equimolar amount of an irrelevant rhIgG1 (data not shown). In the Matrigel tubule formation assay, OXB-203E vector-derived aflibercept significantly inhibited HUVEC total tubule length compared to OXB-Null supernatant (Figure 3B; $p = 0.0004$). This inhibition was again comparable to that for recombinant aflibercept.[42] The two negative controls for this assay, OXB-Null and IgG1, showed similar and higher inhibition on tubule

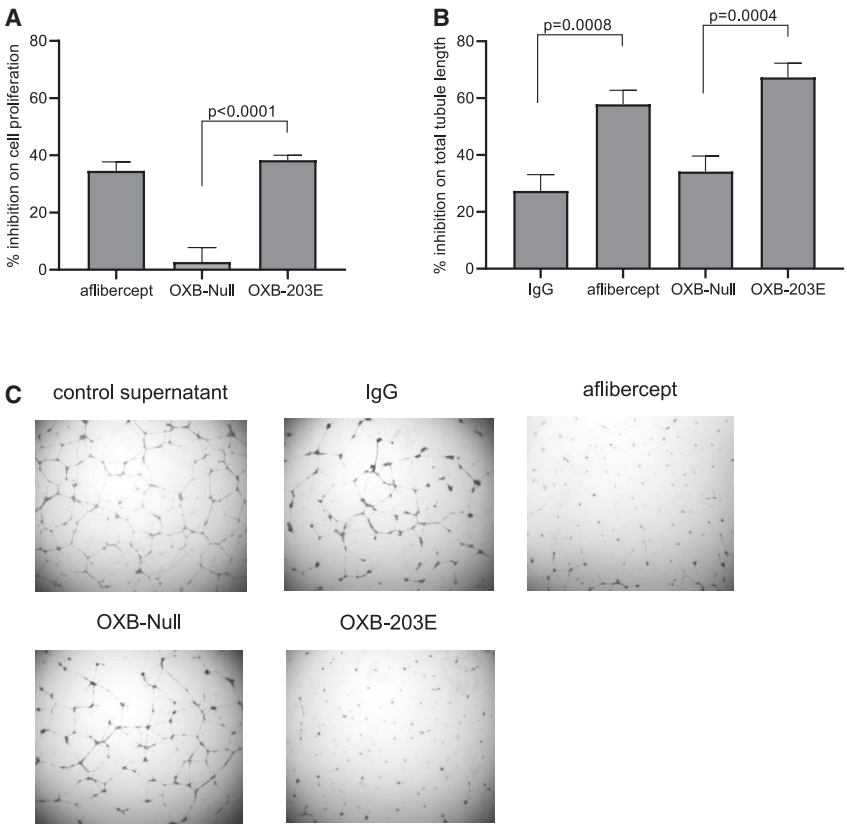

Figure 3. *In vitro* assessment of the biological potency of OXB-203E vector-derived aflibercept

Percentage inhibition of 0.5 nM vector-derived aflibercept on (A) HUVEC proliferation (n = 2) and (B) total tubule length (n = 3) relative to inhibition with supernatant from untransduced cells. Bars represent means from two or three independent assays analyzed in triplicate. Error bars indicate SEM. One-way ANOVA was used to determine significance, and p values are shown where the probability of the result, not assuming null hypothesis, is equal to or less than 0.05. (C) Representative images of HUVEC tubules cultured with control supernatant from untransduced cells, supernatant from OXB-Null transduced cells, an IgG control for recombinant aflibercept, and 0.5 nM aflibercept from OXB-203E transduced cells and recombinant aflibercept.

formation than expected when compared to the proliferation assay. However, despite this inhibition, there was a significantly higher inhibition on tubule length with OXB-203E vector-derived aflibercept and recombinant aflibercept compared to the respective negative controls.

These results demonstrate that OXB-203 vector-derived aflibercept was analogous to recombinant aflibercept; the proteins were of similar molecular weight, both have similar binding characteristics to their target, and OXB-203E vector-derived aflibercept inhibited VEGF-induced HUVEC proliferation and tubule formation similarly to recombinant aflibercept.

In vivo efficacy of OXB-203E

Subretinal administration of OXB-203E at 7 weeks post dosing was compared to an IVT bolus of recombinant aflibercept at 3 weeks post dosing in a rat laser-induced CNV model of nAMD. No adverse events were observed in any of the treated animals throughout the study duration. The mean CNV lesion area for the OXB-203E + buffer group was reduced significantly ($p = 0.019$) compared to the control OXB-Null + buffer group (Figure 4A). The CNV lesion areas for the OXB-203E + buffer group and the OXB-Null + recombinant aflibercept group were comparable, with no significant difference, and this was also reflected in the percentage reduction in the CNV areas relative to the negative control (Figure 4B), where both of these groups showed a 23% reduction compared to the OXB-Null + buffer group. The percentage reduction (±SEM) for the OXB-Null + aflibercept group was 23.2% ± 4.8%, and for the OXB-203E + buffer group, this was 22.9% ± 11%.

To compare the distribution of aflibercept in the eye following subretinal dosing of OXB-203E and IVT dosing of recombinant aflibercept, the vitreous humor, choroid with retinal pigment epithelium (RPE), and retina were harvested *post-mortem*, and aflibercept levels were quantified by ELISA in these tissues. There were significantly higher ($p < 0.0001$) levels of aflibercept in the vitreous and tissues of the OXB-203E + buffer group compared to the OXB-Null + recombinant aflibercept group (Figures 4D–4F). In the vitreous humor, the median aflibercept levels were 1.50 μg/mL (0.75–2.19 μg/mL) for the OXB-203E + buffer group compared to 0.037 μg/mL (0.021–0.043 μg/mL) for the OXB-Null + recombinant aflibercept group, where only 5 out of 16 samples showed quantifiable levels of aflibercept in this group (Figure 4D). In the choroid with RPE, median levels in the two groups were 15.74 μg/g (5.36–41.02 μg/g) and 0.20 μg/g (0.11–0.25 μg/g), respectively (Figure 4E). And in the retina, median levels in the two groups were 13.47 μg/g (8.64–40.89 μg/g) and 0.85 μg/g (0.42–1.15 μg/g), respectively (Figure 4F). There were higher than expected levels of aflibercept (0.22–0.69 μg/g) observed in the choroid with RPE and retinal tissues (Figures 4E and 4F) from the OXB-Null + buffer group which were comparable ($p > 0.99$) to the levels observed from the OXB-Null + recombinant aflibercept group.

These results indicate that a single subretinal dose of OXB-203E was as efficacious in reducing laser-induced CNV as an IVT bolus of recombinant aflibercept. Additionally, OXB-203E vector-derived aflibercept expression in the ocular tissues was at significantly higher levels at 7 weeks post vector dosing compared to the levels from an IVT bolus of recombinant aflibercept at 3 weeks post dosing.

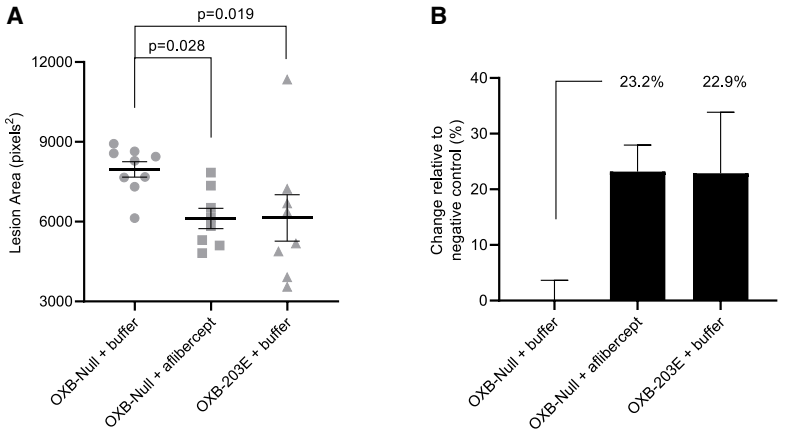

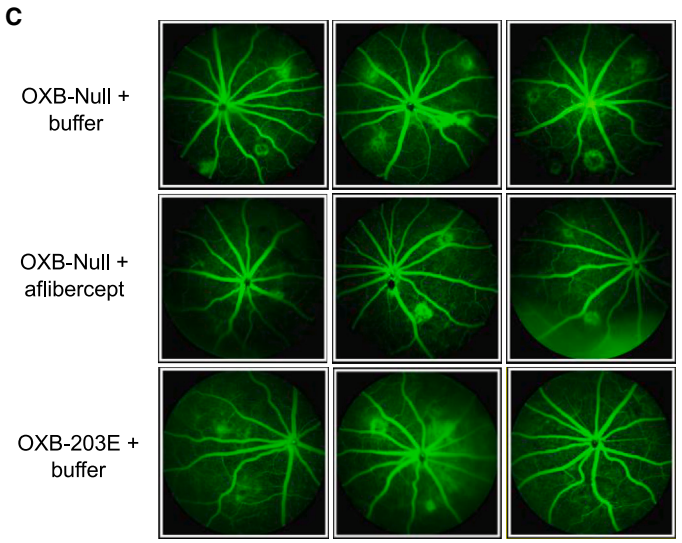

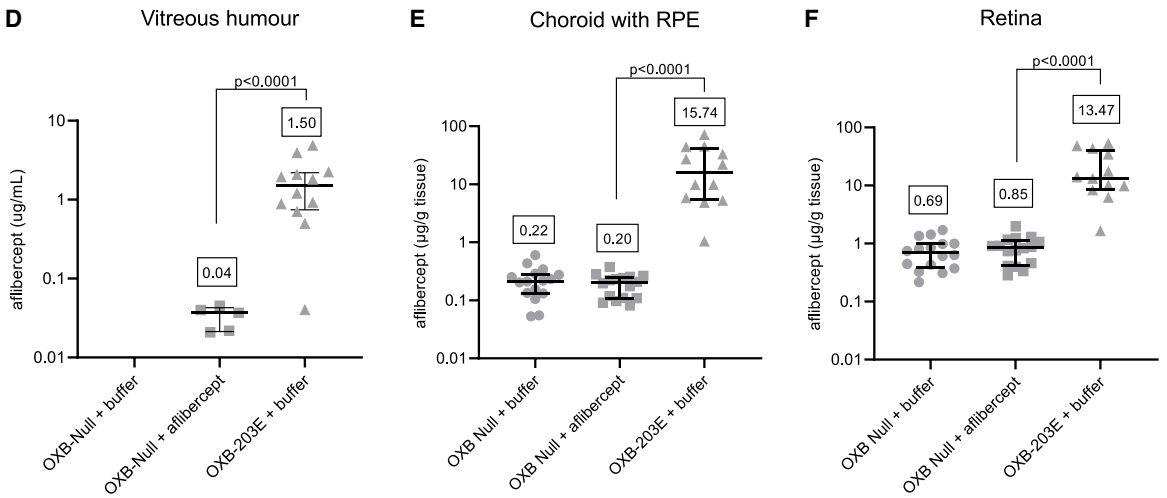

(legend on next page)

Platform comparison study of OXB-203 and AAV8-aflib

The dose selection for OXB-203 and AAV8-aflib for this study was based on the allometric scaling of clinical doses for a subretinally administered lentiviral vector (RetinoStat®)[36] and an AAV (Regenxbio's RGX-314)[43] for nAMD and on the premise that the rat eye is estimated to be one-third the size of a human eye.[44]

Ocular expression of aflibercept from lentiviral and AAV vectors was evaluated in rats 4 weeks following subretinal administration of the vectors. The following 1in 5 diluted vector doses (vector particles [vp]) were injected per rat eye: OXB-Null at 1.07×10^9 vp, OXB-203E at 5.07×10^8 vp, OXB-203H at 2.69×10^8 vp, and AAV8-aflib at 4.65×10^{10} vp (equivalent to genome copies). No adverse events were observed in any of the vector treated animals throughout the study duration.

Administration of either OXB-203H or OXB-203E resulted in significantly higher levels of vector-derived aflibercept compared to AAV8-aflib (at a 100-fold higher vp dose) in most of the ocular tissues analyzed. In the vitreous humor, the median levels of aflibercept from the OXB-203H and OXB-203E treated groups were 9.24 μg/mL (1.06–10.97 μg/mL) and 2.97 μg/mL (1.08–4.60 μg/mL), respectively, both of which were significantly higher ($p = 0.0009$ and 0.0357, respectively) compared to levels from the AAV8-aflib treated group at 0.23 μg/mL (0.05–0.40 μg/mL) (Figure 5A). In the choroid with RPE, the median levels of aflibercept from the OXB-203H and OXB-203E treated groups were 15.45 μg/g (2.04–42.57 μg/g) and 6.85 μg/g (1.47–31.95 μg/g), both of which were also significantly higher ($p = 0.009$ and 0.02, respectively) compared to the AAV8-aflib treated group at 0.79 μg/g (0.31–1.17 μg/g) (Figure 5B). Finally, in the retina, only the median level of aflibercept from the OXB-203H treated group, 22.23 μg/g (3.09–44.75 μg/g), was significantly higher ($p = 0.003$) compared to the AAV8-aflib treated group at 1.33 μg/g (0.92–3.30 μg/g) (Figure 5C). In all three vector platforms, aflibercept concentrations in the choroid with RPE and retina were 2- to 6-fold higher compared to the levels quantified in the vitreous humor. There were no significant differences between the median levels of OXB-203H and OXB-203E vector-derived aflibercept expression in any of the ocular tissues tested. Additionally, evaluation of the aflibercept levels per TU of lentiviral vector administered showed that comparable levels per TU were expressed from both vectors in the vitreous humor (Figure 6A), choroid with RPE (Figure 6B), and retina (Figure 6C).

To compare the aflibercept productivity from the three platforms, the dose of lentiviral (RNA copy number) and AAV (genome copy number) vectors administered were converted to vp (as described in Materials and methods). As animals in the study were dosed with a range of vp, the aflibercept expression per 10^9 vp in each of the tissues was determined as a means of normalizing the data and aiding comparison. Initially, an *in vitro* experiment was conducted to evaluate aflibercept expression from HEK293T cells transduced with increasing doses of matched vp of each vector. OXB-203H and OXB-203E vector-derived aflibercept expression was shown to be significantly higher ($p = 0.005$) compared to AAV8-aflib at each of the matched dose of vp tested (Figure 7A); aflibercept from the AAV vector was only detectable (just above the lower limit of quantification [LLOQ] of the ELISA) at the highest vp dose. HEK293T cells were transduced with similar vp doses of OXB-Null and HIV-Null as negative controls, with no detectable levels of aflibercept observed in the culture supernatants (data not shown).

Evaluation of the *in vivo* expression of vector-derived aflibercept per 10^9 vp in the ocular tissues showed a trend similar to that observed *in vitro*. Aflibercept expression levels were significantly higher ($p < 0.03$) in the vitreous humor (Figure 7B), choroid with RPE (Figure 7C), and retina (Figure 7D) from OXB-203H and OXB-203E treated animals compared to those from AAV8-aflib treated animals. OXB-203 vector-derived aflibercept per 10^9 vp was 420- to 3,400-fold higher in these tissues compared to those from AAV8-aflib. There were no significant differences between OXB-203H and OXB-203E vector-derived aflibercept expression in any of the tissues; however, levels of OXB-203H vector-derived aflibercept were generally higher compared to those from OXB-203E. These results indicate that aflibercept productivity from OXB-203 was superior to AAV.

DISCUSSION

Ongoing gene therapy clinical trials with AAV vectors encoding an anti-VEGF such as aflibercept (Adverum Biotechnologies' ADVM-022 [Ixo-vec]) or anti-VEGFfab (Regenxbio's RGX-314) have shown the merit of this type of treatment for nAMD in terms of providing sustained, long-term expression of vector-derived anti-VEGF with a single administration, significantly reducing the dosing frequency and the associated risks for patients on the current standard of care.

Figure 4. *In vivo* efficacy of OXB-203E in a rat laser-induced CNV model of nAMD

Brown Norway rats received bilateral subretinal injections of 6.90×10^4 TU (1.07×10^9 vp) per eye of OXB-Null (n = 8/9) or 3.30×10^5 TU (2.54×10^9 vp) per eye of OXB-203E (n = 8). Laser-induced CNV lesions were created 4 weeks post dosing, and 2 days later, animals received bilateral IVT injections of TSSM buffer or 0.2 mg recombinant aflibercept per eye. CNV lesion areas and aflibercept concentrations in ocular tissues were quantified at 7 weeks post subretinal administration of vectors. (A) CNV lesion areas (pixels^2) determined by fluorescein angiography. Each symbol represents the mean lesion area for each animal (both eyes), and error bars indicate SEM. One-way ANOVA was used to determine significance. (B) Percentage reduction in the lesion area relative to the OXB-Null + buffer group. (C) Representative fluorescein fundus angiographs showing CNV lesions from each animal group at 7 weeks post subretinal administration of vector. (D–F) Aflibercept concentrations in the (D) vitreous humor, (E) choroid with RPE, and (F) retina. Each symbol represents the aflibercept concentration per eye, with median values and error bars indicating interquartile range (IQR). Nonparametric analysis was performed using Kruskal-Wallis and Dunn's multiple-comparisons tests, and p values are shown where the probability of the result, not assuming Null hypothesis, is equal to or less than 0.05.

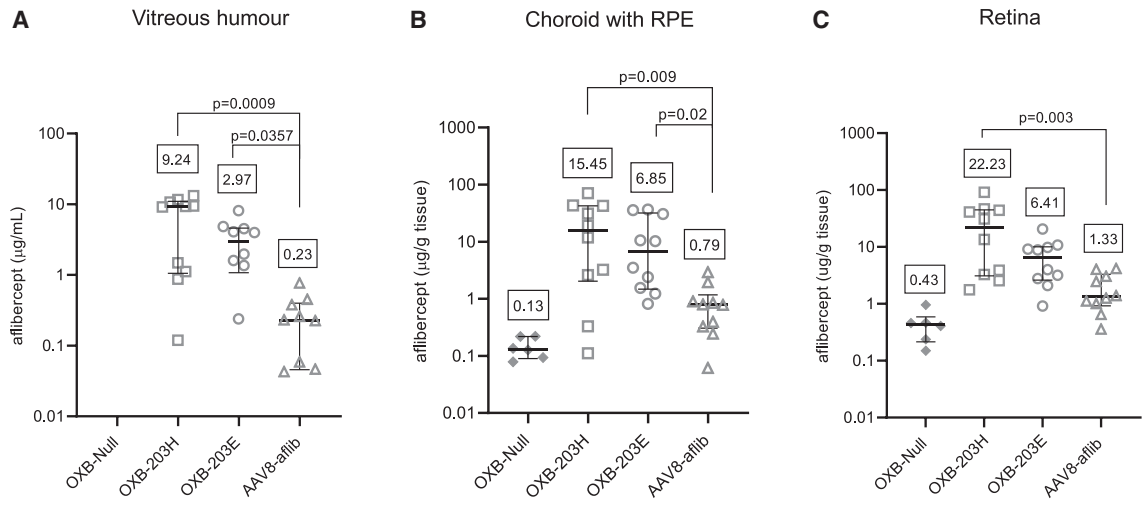

Figure 5. Evaluation of aflibercept expression in rat ocular tissues 4 weeks post subretinal administration of vectors

OXB-203 and AAV8-aflib were dosed at the following vp per eye to rats: OXB-Null at 1.07×10^9 vp (n = 3), OXB-203H at 2.69×10^8 vp (n = 5), OXB-203E at 5.07×10^8 vp (n = 5), and AAV8-aflib at 4.65×10^{10} vp (n = 5). (A–C) Vector-derived aflibercept was quantified in (A) vitreous humor, (B) choroid with RPE, and (C) retina. Each symbol represents the aflibercept concentration for each eye, with median values and error bars indicating IQR. Nonparametric analysis was performed using Kruskal-Wallis and Dunn's multiple-comparisons tests, and p values are shown where the probability of the result, not assuming Null hypothesis, is equal to or less than 0.05.

In our study, we describe the therapeutic potential of a lentiviral-based gene therapy vector for nAMD, EIAV (OXB-203E) and HIV-1 (OXB-203H) encoding aflibercept. *In vitro* assessment of the biochemical function of OXB-203 vector-derived aflibercept demonstrated its ability to bind and block the activity of rhVEGFA$_{165}$, which was comparable to that of recombinant aflibercept. The equivalent binding affinities of OXB-203E vector-derived aflibercept and recombinant aflibercept to rhVEGFA$_{165}$, also translated to its *in vitro* biological potency, where comparable inhibition of VEGF-induced cell proliferation and tubule formation were observed with both proteins in two commonly used angiogenesis assays.[45] Activation of VEGFR2 by VEGFA, necessary for many critical types of physiological and pathological angiogenesis, upregulates nitric oxide synthase, which promotes vascular endothelial cell proliferation,[46] and blockade of VEGFA binding to VEGFR2 by aflibercept inhibits this process. The configuration of aflibercept facilitates binding to VEGFA with greater affinity than binding of VEGFA to VEGFR1 and VEGFR2,[47] enabling efficient VEGF neutralization by aflibercept.

OXB-203 vector-derived aflibercept, when analyzed by Western blot (Figure 2B), was of the expected size relative to recombinant aflibercept. However, an unexpected band of higher molecular weight was observed for recombinant aflibercept. Recombinant aflibercept manufactured using Chinese hamster ovary (CHO) cells, is a dimeric glycoprotein containing several glycosylation sites on each polypeptide chain, and under reducing conditions, this protein migrates as a major band of ~70 kDa (where the disulfide bonds of the IgG1 Fc hinge region are disrupted),[48,49] with two additional minor bands observed with molecular weights of ~55 kDa and 45 kDa in SDS-PAGE analysis.[48] It is possible that the higher molecular weight protein product that was observed, represents the heterogeneity in the glycosylation profile of this recombinant protein; however, this needs to be confirmed using glycosylation inhibition or de-glycosylation assays.

Evaluation of the *in vitro* potency of OXB-203E in a VEGF-induced HUVEC proliferation and Matrigel tubule formation assays demonstrated that OXB-203E vector-derived aflibercept significantly inhibited cell proliferation and tubule formation compared to the negative controls (Figure 3). However, the OXB-Null and IgG1 negative controls for the Matrigel assay showed higher inhibition on tubule formation than expected compared to the proliferation assay. This could be due to several variables; e.g., a different operator performing each assay and variations in the time point of analysis for these assays following cell seeding (18 h for the Matrigel assay compared to 72 h for the proliferation assay).

In the rat CNV model of nAMD, administration of a single subretinal dose of OXB-203E proved to be as efficacious in reducing CNV lesion areas as an IVT bolus of recombinant aflibercept. This result was analogous to the pre-clinical data reported with Adverum Biotechnologies' ADVM-022 (AAV2.7m8-aflibercept) in a non-human primate (NHP) model of nAMD,[25] where an AAV vector delivering aflibercept as a transgene showed no statistical difference in the reduction of CNV lesions compared to aflibercept delivered as a recombinant protein. Fluorescein angiography was utilized to measure CNV lesion areas rather than the conventional method (i.e., *ex vivo* analysis of CNVs on immunolabelled choroidal flat mounts) as the ocular tissues (choroid with RPE and retina) were required for the evaluation of aflibercept expression. This alternative method for CNV area measurement has been shown to correlate with data obtained from choroidal flat mounts.[50] In terms of transgene expression in the ocular tissues, OXB-203E vector-derived aflibercept levels were significantly higher

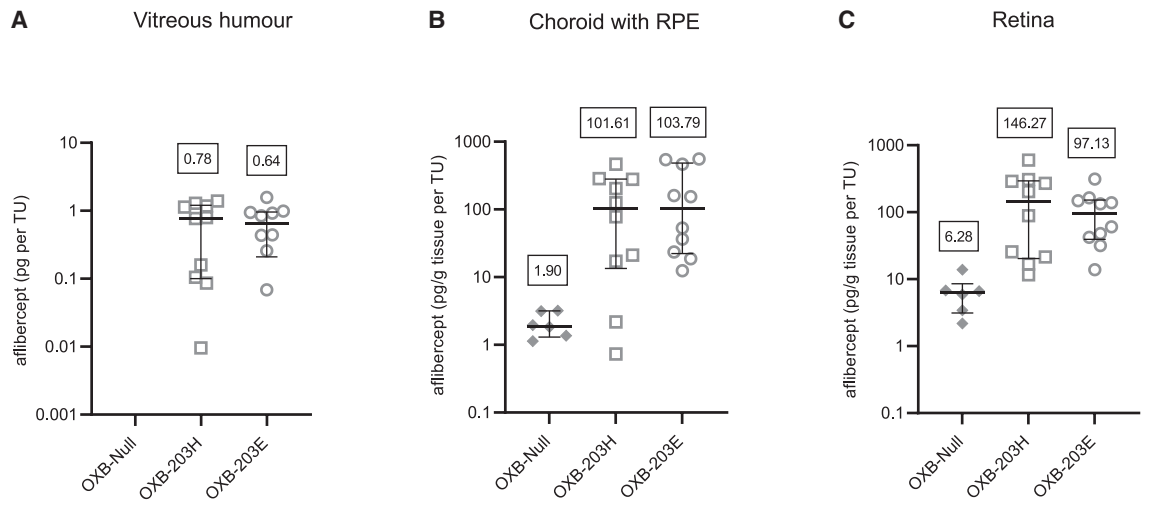

Figure 6. Comparison of expression of OXB-203H and OXB-203E vector-derived aflibercept per TU of vector in rat ocular tissues 4 weeks post subretinal administration of vectors

Vectors were dosed at the following TU per eye to rats: OXB-Null at 6.90×10^4 TU (n = 3), OXB-203H at 1.52×10^5 TU (n = 5), and OXB-203E at 6.60×10^4 TU (n = 5). (A–C) Vector-derived aflibercept, picograms (pg) per TU, was quantified in (A) vitreous humor, (B) choroid with RPE, and (C) retina. Each symbol represents the concentration for each eye, with median values and error bars indicating IQR. Nonparametric analysis was performed using Kruskal-Wallis and Dunn's multiple-comparisons tests.

compared to those from an IVT bolus of recombinant aflibercept. Recombinant aflibercept has a half-life of 115 h in the vitreous humor,[51] which leads to a decrease in its bioavailability over time. In contrast, sustained expression of vector-derived aflibercept is likely to be maintained in the tissues following subretinal administration of OXB-203E directly targeting the RPE and retina. Higher than expected levels of aflibercept (>0.2 μg/g) were observed in the choroid with RPE and retinal tissues (Figures 4E and 4F) of animals treated with OXB-Null + buffer. It has been reported that receptors in adult rat tissues can bind to $rhVEGFA_{165}$ and that these binding sites are associated with endothelial cells.[52] $RhVEGFA_{165}$ was used as the coating protein for the detection of aflibercept by ELISA, and this may potentially bind to receptors found in rat choroidal and retinal endothelial cells with subsequent non-specific binding of the receptors to the ELISA's secondary IgG horseradish peroxidase (HRP) antibody, contributing to the background levels observed in the control tissues.

The *in vitro* and *in vivo* efficacy of OXB-203 was only evaluated with the EIAV platform (OXB-203E) and not with HIV-1 (OXB-203H) as both lentiviral vector-derived aflibercept showed similar binding affinities to VEGF as recombinant aflibercept. This was as expected given that the two vectors had identical expression cassettes and aflibercept open reading frames; therefore, only the potency of OXB-203E was determined. As such, the data that was generated for the *in vivo* platform comparison study demonstrated that OXB-203E and OXB-203H were comparable in terms of aflibercept productivity per TU dosed (Figure 6), indicating that both vectors could be equally efficacious.

When applying a viral vector-based gene therapy approach for treatment of nAMD, careful consideration should be given to the route of administration. The current anti-VEGF treatments for patients with nAMD (aflibercept,[7] ranibizumab, and bevacizumab[53]), when delivered intravitreally, offer a greater drug concentration in the vitreous and inner retina,[54,55] and is a common route of delivery due to the simplicity of the procedure. A major drawback of this route when using a vector-based gene therapy approach is the presence of the inner limiting membrane (ILM). This ILM separates the vitreous from the neural retina and acts as a physical barrier to vector diffusion across the eye sub-compartments.[56] Additionally, intravitreally administered viral vectors are diluted immediately upon mixing with the vitreous and, situated outside of the immune-privileged retinal compartment, are at increased risk of neutralization.[57,58] On the other hand, delivery of viral vectors directly to the subretinal space, a closed anatomical area having a greater immune privilege than the vitreous, potentially reduces antigen presentation and trafficking of immune cells and lowers the risk of encountering anti-transgene immune responses.[59] AAV capsids can potentially induce immune responses in the eye, and a short course of immunosuppression may be required until the capsid antigens are cleared from the infected cells.[60] Studies have shown that there is a dose-response relationship between humoral immunity to AAV capsids and the dose of injected AAV particles,[61] which limits the maximum viral particle dose that can be administered and may, in turn, limit the therapeutic benefit in some cases. Comparison of IVT and subretinal delivery of a clinical-grade recombinant AAV vector to NHPs demonstrated that IVT injections were associated with a higher risk of humoral immune responses compared to subretinal injections.[62] Furthermore, gene therapy with recombinant AAV vectors administered subretinally to nAMD patients in clinical trials has been reported to be safe and well tolerated.[32,63,64] An advantage of using subretinal delivery is that it has a direct effect on the resident cells and tissues in the

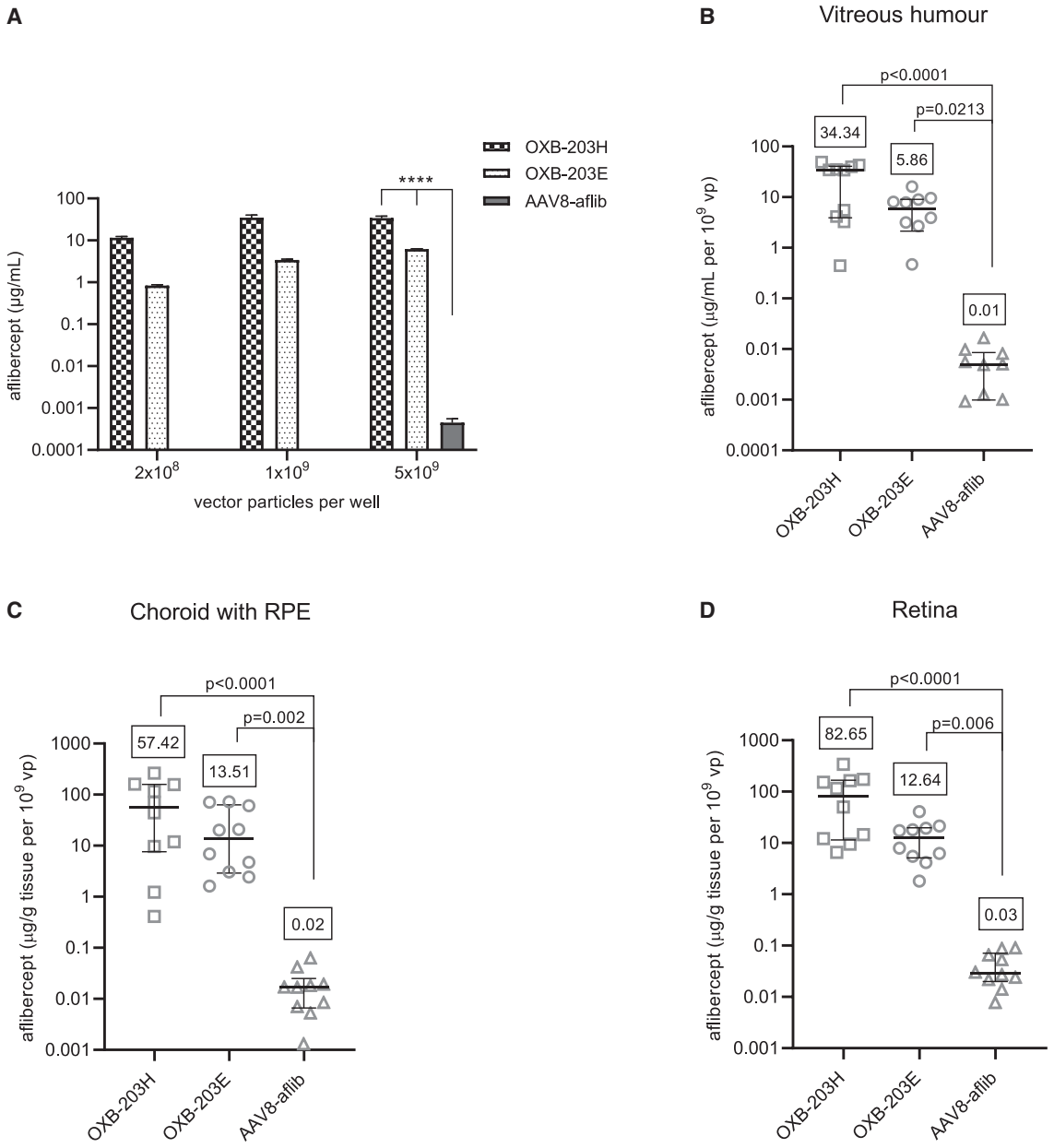

Figure 7. Comparison of expression of vector-derived aflibercept from matched vector particles of OXB-203H, OXB-203E, and AAV8-aflib *in vitro* and *in vivo* following subretinal administration of vectors

(A) Quantification of *in vitro* vector-derived aflibercept in culture supernatants from HEK293T cells transduced with matched vp of OXB-203H, OXB-203E, and AAV8-aflib. Bars indicate means of duplicate transductions, and error bars indicate SD. An asterisk denotes significance. For the *in vivo* study, vectors were dosed at the following vp per rat eye: OXB-203H at 2.69×10^8 vp (n = 5), OXB-203E at 5.07×10^8 vp (n = 5), and AAV8-aflib at 4.65×10^{10} vp (n = 5). (B–D) Vector-derived aflibercept per 10^9 vp was quantified in (B) vitreous humor, (C) choroid with RPE, and (D) retina 4 weeks post subretinal delivery of vectors. Symbols represent the concentration for each eye, with median values and error bars indicating IQR. Nonparametric analysis was performed using Kruskal-Wallis and Dunn's multiple-comparisons tests, and p values are shown where the probability of the result, not assuming Null hypothesis, is equal to or less than 0.05.

subretinal space, and therefore a lower therapeutic dose could be required for accurate targeting of cells. It is well established that subretinal delivery of HIV and EIAV lentiviral vectors consistently results in efficient and stable transduction of RPE cells.[65–67] Moreover, subretinal administration of RetinoStat®, an EIAV-based gene therapy for nAMD, has been reported to be safe and well tolerated, showing scarce or no ocular inflammation in the GEM study (ClinicalTrials.gov: NCT01301443), and immune responses against

Table 1. Vector titers and doses administered for the *in vivo* efficacy and platform comparison studies

Vector titers				Efficacy study		Platform comparison study	
Vector	Titer TU per mL	Titer vp per mL	P:I ratio	TU dosed	vp dosed	vp dosed	TU dosed
OXB-Null	2.30×10^{7}	3.58×10^{11}	1.56×10^{4}	6.90×10^{4}	1.07×10^{9}	1.07×10^{9}	6.90×10^{4}
OXB-203E	1.10×10^{8}	8.45×10^{11}	7.68×10^{3}	3.30×10^{5}	2.54×10^{9}	5.07×10^{8}	6.60×10^{4}
OXB-203H	2.53×10^{8}	4.49×10^{11}	1.77×10^{3}			2.69×10^{8}	1.52×10^{5}
AAV8-aflib	N/A	7.75×10^{13}	N/A			4.65×10^{10}	N/A

Biological titers are presented as transducing units (TU) per mL and physical titers as vector particles (vp) per mL. Vector particle-to-infectivity ratios (P:I) based on these titers are also shown for the lentiviral vectors. For the efficacy study, TU doses of vectors (undiluted) in the 3-μL volume administered subretinally to each rat eye of OXB-Null and OXB-203E are shown, along with the equivalent vp doses. For the platform comparison study, vp doses of vectors (diluted 1 in 5 in TSSM buffer) in the 3-μL volume administered subretinally to each rat eye of OXB-Null (undiluted), OXB-203, and AAV8-aflib are shown, along with the equivalent TU doses. N/A, not applicable as the biological titer and P:I ratio were not determined for AAV8-aflib. All doses were rounded up to 2 decimal points following calculations.

RetinoStat® were not detected in serum or aqueous humour samples from these patients.[36] Biodistribution analysis in rabbits demonstrated that subretinally administered RetinoStat® was maintained within the ocular compartment and was not detected in other organs.[68] As such, OXB-203 should be equally safe and well tolerated in patients.

Gene therapy for nAMD with different viral vector types vary in their clinical dosing; a lentiviral vector dose is based on TU per eye (RetinoStat®),[36] whereas an AAV dose is based on genome copies per eye (Ixo-vec and RGX-314).[29,43] Consequently, OXB-203 and AAV8-aflib doses for the platform comparison study were based on the allometric scaling of clinical doses for a subretinally administered lentiviral vector (RetinoStat®)[36] and an AAV (Regenxbio's RGX-314)[43] and on the premise that the rat eye is estimated to be one-third the size of the human eye.[44] RetinoStat® dosed for the GEM study (ClinicalTrials.gov: NCT01301443)[36] ranged from 2.4×10^{4} to 8.0×10^{5} TU per eye. The 1 in 5 diluted doses administered for OXB-203E at 5.07×10^{8} vp per eye and OXB-203H at 2.69×10^{8} vp per eye when converted to TU dose per eye were 6.60×10^{4} TU for OXB-203E and 1.52×10^{5} TU for OXB-203H (Table 1), which were within the 3-fold lower RetinoStat® dose range for rats at 8.0×10^{3} to 2.7×10^{5} TU per eye. The clinical dose for RGX-314, currently in a Phase I/II study,[43] range from 3×10^{9} to 2.5×10^{11} genome copies/ vector particles (vp) per eye; therefore, the 1 in 5 diluted AAV8-aflib dose at 4.65×10^{10} vp per eye was within the allometrically scaled dose range for rats at 1.0×10^{9} to 8.3×10^{10} vp per eye. Hence, for the platform comparison study, AAV8-aflib was dosed at 100-fold higher vp compared to OXB-203, based on the allometric scaling from clinically relevant doses. Aflibercept expression was evaluated in the ocular tissues of rats subretinally administered with a 1 in 25 diluted dose of AAV8-aflib (9.30×10^{9} vp per eye), and this was found to be 1.5- to 4.5-fold lower (data not shown) compared to the expression from the AAV8-aflib dose of 4.65×10^{10} vp per eye shown here (Figure 5). Retinal toxicity was not assessed with the varying vector doses administered to animals; nevertheless, no adverse events were reported in relation to any of the three vector platforms (OXB-203H, OXB-203E, or AAV8-aflib) during the twice daily observations conducted over the 4-week period prior to study termination. The clinical dose range for RGX-314 on which the AAV8-aflib dose was based has shown nine serious adverse events (SAEs) in patients; however, none were considered to be related to the vector.[43] Additionally, RetinoStat®, on which the OXB-203 doses were based, did not cause any SAEs in the GEM study.[36]

OXB-203 vector-derived aflibercept expression was shown to be significantly higher compared to that from AAV8-aflib (all vectors encode the same aflibercept transgene cassette) both *in vitro* and *in vivo* following a single subretinal administration. This is likely due to lentiviruses being able to stably integrate into the host-cell genome,[69,70] whereas AAVs mainly persist as episomal DNA in cells, which can be diluted over time as the cell replicates, resulting in loss of transgene expression.[71] The aflibercept concentrations in the choroid with RPE and retinal tissues were 2- to 6-fold higher when compared to the levels in the vitreous for all three vector platforms (Figure 5), which would be expected since subretinal delivery directly targets the RPE and retina, the vectors mainly transducing cells in these regions. Conversely, with decreasing doses of IVT ADVM-022 in NHPs, aflibercept concentrations in the choroid were 1.5- to 4-fold lower compared to the vitreous;[26] this mode of delivery limiting AAV transduction in tissues furthermost from the vitreous. Levels of OXB-203H vector-derived aflibercept in the ocular tissues were generally higher though not statistically significant when compared to the levels from OXB-203E. This could be attributed to the differences in the particle-to-infectivity (P:I) ratio for these vectors (Table 1), with OXB-203H having a 4-fold lower P:I ratio (1.77×10^{3}) compared to OXB-203E (7.68×10^{3}), which was reflected in the 4- to 6.5-fold higher levels of aflibercept derived from OXB-203H compared to OXB-203E. Furthermore, when aflibercept expression in each of the ocular tissues was determined based on the transduction efficiency of OXB-203 (i.e., aflibercept per TU of vector dosed), both OXB-203H and OXB-203E showed comparable levels (Figure 6), signifying that both vectors could be equally efficacious. As the integration titer of OXB-203H was 7.7-fold higher compared to OXB-203E when produced using suspension HEK293T cells, this could equate to increased doses being available from OXB-203H in a clinical setting. Evaluation of vector-derived aflibercept expression per 10^{9} vp administered showed significantly higher levels with OXB-203 compared to AAV8-aflib in the ocular tissues assessed, demonstrating superior transgene

expression from the lentiviral vectors compared to AAV (Figure 7). OXB-203 vector-derived aflibercept expression levels in the vitreous from subretinally delivered vectors were comparable to the levels reported in NHPs with intravitreally delivered ADVM-022[26] despite the 2- to 3-log-lower vector dose administered for OXB-203. This indicates that significantly lower doses of OXB-203 may be required to produce comparable levels of aflibercept in the vitreous with a subretinal delivery compared to that from an intravitreally delivered AAV. This dose of ADVM-022 has also been reported to be efficacious in the NHP model of nAMD,[25] and in the OPTIC study, ADVM-022 (Ixo-vec) in patients has been shown to maintain safety and efficacy out to 26 months[28] and stable aflibercept expression out to 3 years.[72] For OXB-203, this potentially represents equivalent or improved outcomes in the clinic with significantly lower therapeutic doses of the lentiviral vectors.

A principal concern when using a viral vector encoding an anti-VEGF is the long-term inhibition of VEGF in the patient. Systemic levels of aflibercept were not detected in the serum of NHPs following IVT administration of ADVM-022,[27] and the OPTIC study (ClinicalTrials.gov: NCT03748784) with ADVM-022 has not reported any adverse events in nAMD patients related to long-term inhibition of VEGF out to 3 years.[72] Conversely, in patients receiving 3 monthly IVT injections of 2 mg recombinant aflibercept, levels of systemic aflibercept were elevated and correlated with a reduction in plasma free-VEGF levels,[73] indicating that sustained expression of vector-derived aflibercept at a targeted therapeutic range is potentially safer compared with a high dose of an IVT bolus of recombinant aflibercept. The potential neuroprotective role of VEGF in retinal ganglion cells may also be affected by its sustained inhibition, leading to the death of photoreceptors. However, continuous blockade of VEGF in mice showed no adverse effects on the retina[74] or choroid,[75] nor did it damage photoreceptors.[76] Long-term expression of aflibercept in the retina from ADVM-022 treated NHPs did not result in retinal toxicity, as evidenced by normal retinal morphology and function at 21 and 30 months.[27,77]

In summary, we have successfully demonstrated the *in vitro* biochemical and functional equivalence of OXB-203 vector-derived aflibercept to recombinant aflibercept. A single subretinal administration of OXB-203E proved to be as efficacious as an IVT bolus of recombinant aflibercept in reducing laser-induced neovascularization. Furthermore, OXB-203 vector-derived aflibercept expression in the eye was shown to be superior to that from an AAV following subretinal delivery of vector doses based on allometric scaling of clinical doses from a subretinally administered lentiviral vector[36] and an AAV[43] for nAMD. Ongoing clinical trials with AAV expressing anti-VEGFs (aflibercept[28,72] and anti-VEGFfab[32,33]) have demonstrated that this approach is safe and well tolerated in nAMD patients. Therefore, our data presented here with OXB-203 and prior data from RetinoStat®, demonstrating safety and sustained, long-term transgene expression with a lentiviral vector,[36] support the therapeutic potential of OXB-203 for the management of nAMD.

MATERIALS AND METHODS

Cell lines

The human embryonic kidney cell line expressing the SV40 large T antigen (HEK293T) and the canine osteosarcoma (D17) cell line were obtained from the ATCC (LGC Standards, Teddington, UK) and cultured in Dulbecco's modified Eagle's medium (DMEM, Merck Life Science, Dorset, UK) supplemented with 10% heat-inactivated fetal bovine serum (FBS; Thermo Fisher Scientific, UK), 2 mM L-glutamine (Merck Life Science) and 1% non-essential amino acids (NEAAs; Merck Life Science). HEK293T cells adapted to culture in suspension phase were maintained in Freestyle™ 293 Expression Medium (FS; Thermo Fisher Scientific) with 0.1% cholesterol lipid concentrate 250× (CLC; Thermo Fisher Scientific) (FS + 0.1% CLC). HUVECs (C-12205, PromoCell, Heidelberg, Germany) prescreened for their proliferative activity with rhVEGFA$_{165}$ were cultured in endothelial growth medium (EGM; C-22110, PromoCell) and passaged following the manufacturer's instructions.

Viral vector construction

The amino acid sequence for aflibercept (DrugBank: DB08885) was reverse translated to cDNA, codon optimized, and synthesized by Thermo Fisher Scientific. It was then cloned into minimal self-inactivating EIAV (OXB-203E) and HIV-1 (OXB-203H) transfer vectors with inclusion of an upstream interleukin-2 (IL-2) secretory signal sequence, a TRAP binding sequence (TBS), transgene repression in vector production (TRiP) system™,[78] an internal human cytomegalovirus (hCMV) promoter driving its expression, and a modified version of the woodchuck hepatitis virus post-transcriptional regulation element (WPRE) downstream of the transgene (Figure 1). The self-complimentary AAV construct encoding the same sequence for the codon-optimized aflibercept with the IL-2 secretory signal, TBS sequence, and hCMV promoter (AAV-aflib) was cloned by VectorBuilder (Chicago, IL, USA). The aflibercept expression cassette was identical in all three vector platforms.

Vector production

OXB-203E, OXB-203H, OXB-Null (EIAV-Null), and HIV-Null vectors pseudotyped with vesicular stomatitis virus-G protein (VSV-G)[79] were produced by transient transfection of either adherent or suspension HEK293T cells. Adherent cells were transfected with vector genome, TRAP, gag-pol packaging, and VSV-G envelope plasmids (and for the HIV-1 vector only, pREV plasmid) using Lipofectamine™ 2000CD (Thermo Fisher Scientific) in 10-cm Petri dishes as described previously[78] and following sodium butyrate (Merck Life Science) induction; the serum containing HEK293T culture medium was replaced with FS + 0.1% CLC. Transfection in HEK293T suspension cells was performed in shake flasks seeded at 9×10^5 cells/mL 24 h prior to transfection and incubated on a shaking platform set at 190 rpm in a 37°C and 5% CO_2 incubator. The plasmid concentrations, and volumes for media (FS + 0.1% CLC), and Lipofectamine™ 2000CD for transfection per mL of suspension cells were as follows: plasmid concentrations: 0.95 μg/mL vector genome, 0.1 μg/mL gag-pol packaging, 0.07 μg/mL VSV-G (0.06 μg/mL REV

for HIV-1 only) and TRAP plasmid at genome-to-TRAP molar ratios of 2:1 for HIV-1 and 5:1 for EIAV. Plasmids were diluted in 62.8 μL medium (FS + 0.1% CLC) per mL of suspension cells. Lipofectamine™ 2000CD for transfection was used at 4.9 μL/mL with 61.7 μL/mL medium (FS + 0.1% CLC). One molar sodium butyrate at 10 μL/mL was added 24 h following transfection, and vector was harvested 24 h following butyrate induction. The viral vectors were concentrated 2,000-fold by double centrifugation, first at 6,000 × *g* for 18–24 h at 4°C in a Beckman mid-speed centrifuge. Vector pellets were then resuspended in phosphate-buffered saline (PBS, Merck Life Science), followed by a second centrifugation at 50,000 × *g* for 1.5 h at 4°C in a Beckman ultracentrifuge and resuspension in a proprietary-formulation buffer Tromethamine, NaCl, Sucrose and Mannitol (TSSM).[80] AAV8-aflib (serotype 8) was produced by VectorBuilder with the AAV-aflib plasmid co-transfected with proprietary Rep-cap and helper plasmids encoding adenovirus genes (E4, E2A, and VA) that mediate AAV replication in adherent HEK293T packaging cells. Following a short incubation period, viral particles were harvested, concentrated by polyethylene glycol (PEG) precipitation, and formulated in a proprietary Tris-based buffer. Lentiviral vectors for all *in vivo* studies were produced using adherent HEK293T cells.

Vector characterization

To determine the integration titer (TU per mL) in HEK293T cells, genomic DNA was extracted from the transduced cells after three consecutive passages over a period of 10 days. DNA extraction was performed on a QIAcube® HT instrument using the QIAamp 96 DNA QIAcube HT Kit (QIAGEN, Manchester, UK). Integrated vector genomes were quantified by duplex qPCR using primers and probe sets specific for EIAV[81] and HIV-1 (fwd, 5′-TGGGCAAGC AGGGAGCTA-3'; rev, 5′- TCCTGTCTGAAGGGATGGTTGT-3′; probe, 5′-FAM-AACGATTCGCAGTTAATCCTGGCCTGTT-TAM ARA-3′) packaging signal and a cellular gene, ribonuclease P RNA component H1 (RPPH1) on a QuantStudio™ 6 Flex real-time PCR system (Thermo Fisher Scientific). To determine the vector RNA copy number, RNA was extracted from the lentiviral vectors using the QIAamp Viral RNA Mini Kit (QIAGEN) with DNase treatment and quantified by qRT-PCR using the same sequences of EIAV and HIV-1 primers and probe sets for the packaging signal as above. AAV titration was performed by VectorBuilder with evaluation of genome copies per mL. Briefly, the AAV viral genome was extracted from lysed viral particles, and qPCR was used to quantify the copy number of the viral genome (using the copy number of the inverted terminal repeat (ITR) region as a proxy) in the stock.

Comparison of aflibercept productivity from OXB-203 and AAV8-aflib

To compare the aflibercept productivity of lentiviral vectors with AAV, the concentration of vp dosed was determined. The lentiviral genome consists of two single-stranded RNA molecules enclosed in the core of the viral vp. Therefore, the RNA copy number, evaluated by qRT-PCR (described above), was divided by two to obtain an approximation of vp. For AAV, each genome copy will be contained in a viral vp; hence, the AAV titer of genome copies equates to vp.

In vitro production of vector-derived aflibercept

HEK293T cells were seeded in 12-well plates and transduced with matched MOI of OXB-203H and OXB-203E or matched vp of OXB-203 and AAV8-aflib. Transduction with lentiviral vectors was performed in the presence of 8 μg/mL polybrene (Merck Life Science) and for AAV8-aflib in the absence of serum and polybrene. Cells were transduced for a period of 4 h, after which medium containing serum was added. Three days following transduction, supernatants were collected and tested for the presence of aflibercept as described below. OXB-203 integrated VCNs were determined as described above, 10 days post transduction.

To generate vector-derived aflibercept for use in the HUVEC proliferation and tubule formation assays, D17 cells were transduced as described above and cultured in DMEM containing 2% FBS, 2 mM L-glutamine, and 1% NEAAs. Culture supernatants were harvested, filtered, aliquoted, and frozen at −80°C.

Anti-VEGFA ELISA and western blot

Measurements of aflibercept protein levels in culture supernatants were performed with an anti-VEGFA ELISA. Immunolon 4HBX 96-well flat-bottomed plates (Thermo Fisher Scientific) were coated with 2 μg/mL of rhVEGFA$_{165}$ (Bio-Techne, Abingdon, UK) in 0.2 M sodium carbonate/bicarbonate buffer (Merck Life Science) and incubated for 2 h at room temperature. After removal of the coating solution, the plates were washed 3 times with wash buffer (PBS containing 0.05% Tween 20, Merck Life Science) and blocked with wash buffer containing 2% bovine serum albumin (BSA, Merck Life Science) for 2 h at room temperature. Culture supernatants and a recombinant aflibercept standard curve (25–0.78 ng/mL) were prepared by dilution in DMEM with either 10% or 2% FBS depending on the level of serum present in the samples to be tested. The blocking buffer was removed, replaced with replicate standards or samples, incubated for 1 h at room temperature on an orbital shaker, and washed 4 times with wash buffer following incubation. Goat anti-human IgG H&L HRP (ab209702, Abcam, Cambridge, UK) diluted 1:20,000 in sample diluent was added and incubated for 2 h at room temperature, and plates were washed. 3,3',5,5'-Tetramethylbenzidine (TMB) ELISA substrate solution (Abcam) was added, and following appropriate color development, the reaction was stopped with an equal volume of stop solution (Abcam). Absorbance at 450 nm (optical density 450 [OD$_{450}$]) was determined using a SpectraMax plate reader (Molecular Devices, San Jose, CA, USA). Standard curves were plotted, and aflibercept concentrations were determined using linear regression in Microsoft Excel.

Vector-derived aflibercept was analyzed by SDS-PAGE and Western blot under reducing conditions using a goat anti-human IgG-HRP antibody (sc-2453, Santa Cruz Biotechnology, Heidelberg, Germany).

VEGF binding assay

This assay was performed as described previously.[47,82] Briefly, 10 pM of rhVEGFA$_{165}$ was incubated overnight at room temperature with increasing concentrations (0.1–160 pM) of vector-derived aflibercept.

Unbound VEGF was measured using a human $VEGFA_{165}$ ELISA kit (Bio-Techne). IC_{50} values were calculated using a sigmoidal 4PL interpolation model in GraphPad Prism software.

VEGF saturation binding assay

Aflibercept from vector-transduced HEK293T cells was purified using Spin Trap columns (GE Healthcare, UK) according to the manufacturer's instructions. Quantification of the purified aflibercept was performed using ELISA as described previously. Plates were coated with 10 nM of vector-derived aflibercept or recombinant aflibercept and incubated for 1 h at room temperature, followed by addition of biotinylated $rhVEGFA_{165}$ from 0.25–10 nM and further incubation for 1 h at room temperature. Following 3 washes with wash buffer, a 1:200 dilution of HRP-conjugated streptavidin (N100, Thermo Fisher Scientific) was added, and the plates were incubated for 1 h at room temperature and washed. TMB ELISA substrate solution was then added and following appropriate color development, the reaction was stopped with an equal volume of Stop solution. OD_{450} was determined as described above. B_{max} and K_d values were calculated using GraphPad Prism software based on the OD_{450}.

In vitro angiogenesis assays

Proliferation assay

Vector-derived aflibercept, recombinant aflibercept, and rhIgG1 (ab158745, Abcam) were diluted in D17 culture supernatant containing 20 ng/mL of $rhVEGFA_{165}$ to a concentration of 0.5 nM and plated onto 96-well flat-bottomed plates in replicates. Following a 2-h incubation at 37°C and 5% CO_2, 2,500 HUVECs/well were added and cultured for 72 h at 37°C and 5% CO_2. The CellTiter-Glo® luminescent cell viability assay (Promega, Southampton, UK) was used to measure cell proliferation[83] on a SpectraMax plate reader following the manufacturer's instructions. Percentage inhibition of cell proliferation relative to inhibition with untransduced D17 control supernatant was calculated.

Matrigel tubule formation assay

Pre-chilled, 96-well, flat-bottomed plates were coated with Matrigel (growth factor reduced, phenol red free; Scientific Laboratory Supplies, Nottingham, UK) and left to polymerize for 1 h at 37°C and 5% CO_2. HUVECs were seeded onto the Matrigel at 1.5×10^4 cells/well. Vector-derived aflibercept, recombinant aflibercept, and rhIgG1 were diluted in untransduced D17 culture supernatant containing 20 ng/mL of $rhVEGFA_{165}$ to a concentration of 0.5 nM and added to the plated HUVECs. Plates were incubated for 18 h at 37°C and 5% CO_2, after which bright-field images were taken using a digital camera mounted on a Carl Zeiss microscope. Analysis of the images was carried out by Onimagin Technologies (Cordoba, Spain) using the Wimasis software, and percentage inhibition of vector-derived aflibercept on HUVEC total tubule length relative to inhibition with untransduced D17 control supernatant was calculated.

Animals for in *vivo studies*

All studies were carried out at EyeCRO (Oklahoma City, OK, USA) using female brown Norway rats on post-natal day 42 (P42); the rats were maintained humanely with institutional approval and in accordance with the Association for Research in Vision and Ophthalmology Statement for the Use of Animals in Ophthalmic and Vision Research, and experiments were performed under an approved institutional animal care and use committee (IACUC) protocol. Animals were housed in groups of 3–5 in large cages kept on ventilated shelves under standard animal care conditions in an environmentally controlled climate of 19°C–21°C and normal humidity on a 16/8-h light/dark cycle. All animals were ear tagged, provided with food and water *ad libitum*, and observed at least twice daily for morbidity, mortality, and injury.

In vivo *efficacy study design*

Animals were randomized and dosed with bilateral subretinal injections of undiluted vectors: groups A (n = 9) and B (n = 8), 6.90×10^4 TU (1.07×10^9 vp) per eye of OXB-Null; group C (n = 8), 3.30×10^5 TU (2.54×10^9 vp) per eye of OXB-203E. Laser-induced CNV lesions were created 4 weeks post dosing, and 2 days later, animals received bilateral IVT injections of TSSM buffer[80] (groups A and C) or 0.2 mg recombinant aflibercept per eye (group B). Fluorescence angiography was used to measure the size of the CNV lesions at 3 weeks post dosing, and following these measurements, animals were euthanized, and the vitreous humor, choroid with RPE, and retina were harvested for quantification of aflibercept.

In vivo *platform comparison study design*

Animals were randomized and dosed with bilateral subretinal injections of vectors diluted 1 in 5 with TSSM buffer: group A (n = 3), OXB-Null (undiluted) at 1.07×10^9 vp per eye (6.90×10^4 TU); group B (n = 5), OXB-203H at 2.69×10^8 vp per eye (1.52×10^5 TU); group C (n = 5), OXB-203E at 5.07×10^8 vp per eye (6.60×10^4 TU); group D (n = 5), AAV8-aflib at 4.65×10^{10} vp per eye. Animals were euthanized at 4 weeks post dosing, and the vitreous humor, choroid with RPE, and retinas were harvested for quantification of aflibercept.

Subretinal vector administration

Animals were anesthetized with an intramuscular injection of 85 mg/kg ketamine and 14 mg/kg xylazine and their pupils dilated with a combination of cyclopentolate hydrochloride ophthalmic solution 0.1% 30 min prior to treatment and 2.5% phenylephrine 5 min prior to treatment. They were placed onto a regulated heating pad, and images of the posterior pole were visualized under magnification. A 12.7-mm, 30G insulin syringe was used to puncture the cornea just above the corneal limbus, avoiding any contact with the sclera and the lens. The transvitreal bilateral subretinal injections were performed with a 10-μL Hamilton syringe and a 33G blunt needle that was inserted through the corneal puncture, across the vitreous, with the shaft aimed at the back of the eyecup, avoiding any trauma to the lens or iris. A total volume of 3 μL of vector was delivered per eye.

Laser induction of CNV

Animals' eyes were dilated with 1% Cyclogyl solution and protected from light. Following observable dilation, the animals were

anesthetized with ketamine and xylazine. The fundus of sedated animals was observed and recorded using a Micron® IV small animal funduscope (PhoenixMicron, Bend, OR, USA). Laser treatment was performed using a thermal laser that was connected through the Micron IV custom laser attachment. A total of 3 lesions per eye were created using a wavelength of 520 nm. Fundus images were recorded and evaluated to confirm that the laser had successfully produced a bubble through the Bruch's membrane.

IVT administration of recombinant aflibercept

Animals were anesthetized with ketamine and xylazine, and pupils were dilated with topical administration of Cyclogyl and/or tropicamide. Following sedation and pupil dilation, a total volume of 5 μL of recombinant aflibercept or TSSM buffer was injected per eye, into the vitreous at the pars plana, using a Hamilton syringe and a 32G needle.

Fluorescein angiography and data analysis

Animals were first anesthetized with ketamine and xylazine and then received an intraperitoneal injection of a 10% fluorescein sodium solution at 1 μL/g of body weight. Fundus images were captured as 8-bit TIFF files using the Micron® IV and exciter/barrier filters for a target wavelength of 488 nm. Standard color fundus photos were also captured for each eye. Lesions were measured in Adobe Photoshop using the freehand drawing tool and magic wand. Any apparent existing vasculature was excluded from the lesion areas. The individually quantified lesion areas were averaged for each animal, and the resulting values were averaged across each group and represented as mean ± standard error of the mean (SEM).

Tissue collection and processing

At the end of the studies, animals were anesthetized by intraperitoneal administration of ketamine and xylazine and euthanized by intraperitoneal administration of Euthasol®, and eyes were enucleated with individual dissection of the vitreous humor, choroid with RPE, and retina, which were snap frozen in liquid nitrogen and stored at −80°C until processing.

Frozen vitreous was diluted in 10 μL of PBS containing 0.1% BSA, vortexed vigorously, and centrifuged for 10 min at 12,000 rpm and 4°C, and the pelleted insoluble material was discarded. Choroid with RPE and retina were weighed, homogenized in BioMasher tubes (Takara Bio, London, UK) with 50 μL of pre-chilled CelLytic™ MT cell lysis reagent (Merck Life Science)[84] containing protease inhibitor cocktail (Merck Life Science), and centrifuged for 10 min at 12,000 rpm and 4°C, and the pelleted insoluble material was discarded. Aflibercept in the tissue lysates was quantified as described above using PBS with 0.1% BSA to prepare the sample dilutions and the recombinant aflibercept standard curve.

Statistical analysis

Data analysis and generation of graphs was performed using GraphPad Prism v.9 for Windows (GraphPad, San Diego, CA, USA) with descriptive statistics (mean with either SD or SEM and median with interquartile range (IQR) at 25% and 75%). Normality tests were used to evaluate the Gaussian distribution of data. Normally distributed data were analyzed using ordinary one-way ANOVA, and data not normally distributed were analyzed using nonparametric tests (Kruskal-Wallis) and Dunn's multiple-comparisons tests.

DATA AVAILABILITY

The data that support the findings cited in this research article are available from the corresponding author (S.I.) upon request.

ACKNOWLEDGMENTS

The authors wish to acknowledge EyeCRO LLC for performing all *in vivo* studies. We thank Alun Barnard for providing advice on statistical analyses and Robert Powles for managing the samples from the *in vivo* studies. The graphical abstract for this manuscript was created with BioRender.

AUTHOR CONTRIBUTIONS

S.I. designed and conducted *in vitro* experiments, analyzed samples from *in vivo* studies, and prepared the manuscript. D.K.B., G.D., and C.P.K. designed and conducted *in vitro* experiments. C.P.K. and D.M.O. supervised *in vivo* studies. S.E. initiated and supervised the project. E.G., K.A.M., and Y.L. supervised the project and reviewed the manuscript.

DECLARATION OF INTERESTS

The authors declare no competing interests.

REFERENCES

1. Guimaraes, T.A.C.d., Georgiou, M., Bainbridge, J.W.B., and Michaelides, M. (2021). Gene therapy for neovascular age-related macular degeneration: Rationale, clinical trials and future directions. Br. J. Ophthalmol. *105*, 151–157.
2. Wong, W.L., Su, X., Li, X., Cheung, C.M.G., Klein, R., Cheng, C.-Y., and Wong, T.Y. (2014). Global prevalence of age-related macular degeneration and disease burden projection for 2020 and 2040: a systematic review and meta-analysis. Lancet Glob. Heal *2*, e106–e116.
3. Hernández-Zimbrón, L.F., Zamora-Alvarado, R., Ochoa-De La Paz, L., Velez-Montoya, R., Zenteno, E., Gulias-Cañizo, R., Quiroz-Mercado, H., and Gonzalez-Salinas, R. (2018). Age-Related Macular Degeneration: New Paradigms for Treatment and Management of AMD. Oxid. Med. Cell. Longev.
4. Ferris, F.L., Wilkinson, C.P., Bird, A., Chakravarthy, U., Chew, E., Csaky, K., and Sadda, S.R.; Beckman Initiative for Macular Research Classification Committee (2013). Clinical classification of age-related macular degeneration. Ophthalmology *120*, 844–851.
5. Rosenfeld, P.J., Rich, R.M., and Lalwani, G.A. (2006). Ranibizumab: Phase III Clinical Trial Results. Ophthalmol. Clin. North Am. *19*, 361–372.
6. Lynch, S.S., and Cheng, C.M. (2007). Bevacizumab for neovascular ocular diseases. Ann. Pharmacother. *41*, 614–625.
7. Heier, J.S., Brown, D.M., Chong, V., Korobelnik, J.F., Kaiser, P.K., Nguyen, Q.D., Kirchhof, B., Ho, A., Ogura, Y., Yancopoulos, G.D., et al. (2012). Intravitreal aflibercept (VEGF trap-eye) in wet age-related macular degeneration. Ophthalmology *119*, 2537–2548.
8. Holekamp, N.M., Liu, Y., Yeh, W.S., Chia, Y., Kiss, S., Almony, A., and Kowalski, J.W. (2014). Clinical utilization of anti-VEGF agents and disease monitoring in neovascular age-related macular degeneration. Am. J. Ophthalmol. *157*, 825–833.e1.
9. Boulanger-Scemama, E., Querques, G., About, F., Puche, N., Srour, M., Mane, V., Massamba, N., Canoui-Poitrine, F., and Souied, E.H. (2015). Ranibizumab for

exudative age-related macular degeneration: A five year study of adherence to follow-up in a real-life setting. J. Fr. Ophtalmol. *38*, 620–627.

10. Boyle, J., Vukicevic, M., Koklanis, K., and Itsiopoulos, C. (2015). Experiences of patients undergoing anti-VEGF treatment for neovascular age-related macular degeneration: A systematic review. Psychol. Heal. Méd. *20*, 296–310.
11. Mathalone, N., Arodi-Golan, A., Sar, S., Wolfson, Y., Shalem, M., Lavi, I., and Geyer, O. (2012). Sustained elevation of intraocular pressure after intravitreal injections of bevacizumab in eyes with neovascular age-related macular degeneration. Graefe's Arch. Clin. Exp. Ophthalmol. Times *250*, 1435–1440.
12. Day, S., Acquah, K., Mruthyunjaya, P., Grossman, D.S., Lee, P.P., and Sloan, F.A. (2011). Ocular complications after antivascular endothelial growth factor therapy in medicare patients with age-related macular degeneration. Am. J. Ophthalmol. *152*, 266–272.
13. Okada, M., Mitchell, P., Finger, R.P., Eldem, B., Talks, S.J., Hirst, C., Paladini, L., Barratt, J., Wong, T.Y., and Loewenstein, A. (2021). Nonadherence or Nonpersistence to Intravitreal Injection Therapy for Neovascular Age-Related Macular Degeneration: A Mixed-Methods Systematic Review. Ophthalmology *128*, 234–247.
14. Ramakrishnan, M.S., Yu, Y., and VanderBeek, B.L. (2020). Association of Visit Adherence and Visual Acuity in Patients with Neovascular Age-Related Macular Degeneration: Secondary Analysis of the Comparison of Age-Related Macular Degeneration Treatment Trial. JAMA Ophthalmol. *138*, 237–242.
15. Hussain, R.M., Hariprasad, S.M., and Ciulla, T.A. (2017). Treatment Burden in Neovascular AMD: Visual Acuity Outcomes are Associated With Anti-VEGF Injection Frequency. Ophthalmic Surg Lasers Imaging Retin *48*, 780–784.
16. Dugel, P.U., Singh, R.P., Koh, A., Ogura, Y., Weissgerber, G., Gedif, K., Jaffe, G.J., Tadayoni, R., Schmidt-Erfurth, U., and Holz, F.G. (2021). HAWK and HARRIER: Ninety-Six-Week Outcomes from the Phase 3 Trials of Brolucizumab for Neovascular Age-Related Macular Degeneration. Ophthalmology *128*, 89–99.
17. PULSAR study. https://clinicaltrials.gov/ct2/show/NCT04423718.
18. Kang-Mieler, J.J., Dosmar, E., Liu, W., and Mieler, W.F. (2017). Extended ocular drug delivery systems for the anterior and posterior segments: biomaterial options and applications. Expet Opin. Drug Deliv. *14*, 611–620.
19. Adamis, A.P., Brittain, C.J., Dandekar, A., and Hopkins, J.J. (2020). Building on the success of anti-vascular endothelial growth factor therapy: a vision for the next decade. Eye *34*, 1966–1972.
20. Xue, K., Zhao, X., Zhang, Z., Qiu, B., Tan, Q.S.W., Ong, K.H., Liu, Z., Parikh, B.H., Barathi, V.A., Yu, W., et al. (2019). Sustained delivery of anti-VEGFs from thermogel depots inhibits angiogenesis without the need for multiple injections. Biomater. Sci. *7*, 4603–4614.
21. Campochiaro, P.A., Marcus, D.M., Awh, C.C., Regillo, C., Adamis, A.P., Bantseev, V., Chiang, Y., Ehrlich, J.S., Erickson, S., Hanley, W.D., et al. (2019). The Port Delivery System with Ranibizumab for Neovascular Age-Related Macular Degeneration: Results from the Randomized Phase 2 Ladder Clinical Trial. Ophthalmology *126*, 1141–1154.
22. Yu, Y.J., Mo, B., Liu, L., Yue, Y.K., Yue, C.L., and Liu, W. (2016). Inhibition of choroidal neovascularization by lentivirus-mediated PEDF gene transfer in rats. Int. J. Ophthalmol. *9*, 1112–1120.
23. Cachafeiro, M., Bemelmans, A.P., Samardzija, M., Afanasieva, T., Pournaras, J.A., Grimm, C., Kostic, C., Philippe, S., Wenzel, A., and Arsenijevic, Y. (2013). Hyperactivation of retina by light in mice leads to photoreceptor cell death mediated by VEGF and retinal pigment epithelium permeability. Cell Death Dis. *4*, 7811–e811.
24. Askou, A.L., Benckendorff, J.N.E., Holmgaard, A., Storm, T., Aagaard, L., Bek, T., Mikkelsen, J.G., and Corydon, T.J. (2017). Suppression of Choroidal Neovascularization in Mice by Subretinal Delivery of Multigenic Lentiviral Vectors Encoding Anti-Angiogenic MicroRNAs. Hum. Gene Ther. Methods *28*, 222–233.
25. Grishanin, R., Vuillemenot, B., Sharma, P., Keravala, A., Greengard, J., Gelfman, C., Blumenkrantz, M., Lawrence, M., Hu, W., Kiss, S., and Gasmi, M. (2019). Preclinical Evaluation of ADVM-022. Mol. Ther. *27*, 118–129.
26. Kiss, S., Grishanin, R., Nguyen, A., Rosario, R., Greengard, J.S., Nieves, J., Gelfman, C.M., and Gasmi, M. (2020). Analysis of Aflibercept Expression in NHPs following Intravitreal Administration of ADVM-022, a Potential Gene Therapy for nAMD. Mol. Ther. Methods Clin. Dev. *18*, 345–353.
27. Kiss, S., Bender, K.O., Grishanin, R.N., Hanna, K.M., Nieves, J.D., Sharma, P., Nguyen, A.T., Rosario, R.J., Greengard, J.S., Gelfman, C.M., et al. (2021). Long-term safety evaluation of continuous intraocular delivery of aflibercept by the intravitreal gene therapy candidate ADVM-022 in nonhuman primates. Transl. Vis. Sci. Technol *10*, 1–15.
28. ADVM-022 Intravitreal Gene Therapy for Neovascular AMD - Phase 1 OPTIC Study. https://adverum.com/wp-content/uploads/2022/03/OPTIC-Retina-Society-Meeting-Updated-9-30-2021a.pdf.
29. Adverum Biotechnologies Announces First Subject Dosed with Ixo-vec in the Phase 2 LUNA Trial for the Treatment of Wet Age-Related Macular Degeneration (2022). https://investors.adverum.com/news/news-details/2022/Adverum-Biotechnologies-Announces-First-Subject-Dosed-with-Ixo-vec-in-the-Phase-2-LUNA-Trial-for-the-Treatment-of-Wet-Age-Related-Macular-Degeneration/default.aspx.
30. Liu, Y., Fortmann, S.D., Shen, J., Wielechowski, E., Tretiakova, A., Yoo, S., Kozarsky, K., Wang, J., Wilson, J.M., and Campochiaro, P.A. (2018). AAV8-antiVEGFfab Ocular Gene Transfer for Neovascular Age-Related Macular Degeneration. Mol. Ther. *26*, 542–549.
31. Ding, K., Shen, J., Hafiz, Z., Hackett, S.F., Silva, R.L.E., Khan, M., Lorenc, V.E., Chen, D., Chadha, R., Zhang, M., et al. (2019). AAV8-vectored suprachoroidal gene transfer produces widespread ocular transgene expression. J. Clin. Invest. *129*, 4901–4911.
32. Regenxbio announces additional positive interim Phase I/IIa and long-term follow-up data of RGX-314 for the treatment of wet AMD. https://www.prnewswire.com/news-releases/regenxbio-announces-additional-positive-interim-phase-iiia-and-long-term-follow-up-data-of-rgx-314-for-the-treatment-of-wet-amd-301228344.html.
33. REGENXBIO Announces Additional Positive Interim Data from Trials of RGX-314 for the Treatment of Wet AMD (2022). https://www.prnewswire.com/news-releases/regenxbio-announces-additional-positive-interim-data-from-trials-of-rgx-314-for-the-treatment-of-wet-amd-301638557.html.
34. Balaggan, K.S., Binley, K., Esapa, M., MacLaren, R.E., Iqball, S., Duran, Y., Pearson, R.A., Kan, O., Barker, S.E., Smith, A.J., et al. (2006). EIAV vector-mediated delivery of endostatin or angiostatin inhibits angiogenesis and vascular hyperpermeability in experimental CNV. Gene Ther. *13*, 1153–1165.
35. Kachi, S., Binley, K., Yokoi, K., Umeda, N., Akiyama, H., Muramatu, D., Iqball, S., Kan, O., Naylor, S., and Campochiaro, P.A. (2009). Equine infectious anemia viral vector-mediated codelivery of endostatin and angiostatin driven by retinal pigmented epithelium-specific VMD2 promoter inhibits choroidal neovascularization. Hum. Gene Ther. *20*, 31–39.
36. Campochiaro, P.A., Lauer, A.K., Sohn, E.H., Mir, T.A., Naylor, S., Anderton, M.C., Kelleher, M., Harrop, R., Ellis, S., and Mitrophanous, K.A. (2017). Lentiviral vector gene transfer of endostatin/angiostatin for macular degeneration (GEM) study. Hum. Gene Ther. *28*, 99–111.
37. (2008). Aflibercept: AVE 0005, AVE 005, AVE0005, VEGF Trap - Regeneron, VEGF Trap (R1R2), VEGF Trap-Eye. Drugs R D, 261–269.
38. Semeraro, F., Morescalchi, F., Duse, S., Parmeggiani, F., Gambicorti, E., and Costagliola, C. (2013). Aflibercept in wet AMD: Specific role and optimal use. Drug Des. Devel. Ther. *7*, 711–722.
39. Sumner, G., Georgaros, C., Rafique, A., Dicioccio, T., Martin, J., Papadopoulos, N., Daly, T., and Torri, A. (2019). Anti-VEGF drug interference with VEGF quantitation in the R & D systems human quantikine VEGF ELISA kit. Bioanalysis *11*, 381–392.
40. Takahashi, H., Nomura, Y., Nishida, J., Fujino, Y., Yanagi, Y., and Kawashima, H. (2016). Vascular endothelial growth factor (VEGF) concentration is underestimated by enzyme-linked immunosorbent assay in the presence of anti-vegf drugs. Invest. Ophthalmol. Vis. Sci. *57*, 462–466.
41. Torimura, T., Iwamoto, H., Nakamura, T., Abe, M., Ikezono, Y., Wada, F., Sakaue, T., Masuda, H., Hashimoto, O., Koga, H., et al. (2016). Antiangiogenic and Antitumor Activities of Aflibercept, a Soluble VEGF Receptor-1 and -2, in a Mouse Model of Hepatocellular Carcinoma. Neoplasia *18*, 413–424.
42. Kim, I.D., Cave, J.W., and Cho, S. (2021). Aflibercept, a VEGF (Vascular Endothelial Growth Factor)-Trap, Reduces Vascular Permeability and Stroke-Induced Brain Swelling in Obese Mice. Stroke *52*, 2637–2648.
43. Campochiaro, P.A. (2022). Subretinal RGX-314: Phase I/IIa Long-Term Follow-Up Results up to 4 Years. https://www.regenxbio.com/getmedia/1ddb1b73-e398-4366-999d-4ce04562c7dd/RGX-314-AAO2022-SR-LTFU_Peter-C_FINAL_.pdf?ext=.pdf.

44. Lozano, D.C., and Twa, M.D. (2013). Development of a rat schematic eye from *in vivo* biometry and the correction of lateral magnification in SD-OCT imaging. Invest. Ophthalmol. Vis. Sci. *54*, 6446–6455.

45. Stryker, Z.I., Rajabi, M., Davis, P.J., and Mousa, S.A. (2019). Evaluation of angiogenesis assays. Biomedicines *7*, 37.

46. Papapetropoulos, A., García-Cardeña, G., Madri, J.A., and Sessa, W.C. (1997). Nitric oxide production contributes to the angiogenic properties of vascular endothelial growth factor in human endothelial cells. J. Clin. Invest. *100*, 3131–3139.

47. Holash, J., Davis, S., Papadopoulos, N., Croll, S.D., Ho, L., Russell, M., Boland, P., Leidich, R., Hylton, D., Burova, E., et al. (2002). VEGF-Trap: A VEGF blocker with potent antitumor effects. Proc. Natl. Acad. Sci. U. S. A *99*, 11393–11398.

48. Sivertsen, M.S., Jørstad, Ø.K., Grevys, A., Foss, S., Moe, M.C., and Andersen, J.T. (2018). Pharmaceutical compounding of aflibercept in prefilled syringes does not affect structural integrity, stability or VEGF and Fc binding properties. Sci. Rep. *8*, 1–9.

49. Lode, H.E., Gjølberg, T.T., Foss, S., Sivertsen, M.S., Brustugun, J., Andersson, Y., Jørstad, Ø.K., Moe, M.C., and Andersen, J.T. (2019). A new method for pharmaceutical compounding and storage of anti-VEGF biologics for intravitreal use in silicone oil-free prefilled plastic syringes. Sci. Rep. *9*, 1–10.

50. Wigg, J.P., Zhang, H., and Yang, D. (2015). A quantitative and standardized method for the evaluation of choroidal neovascularization using MICRON III fluorescein angiograms in rats. PLoS One *10*. e0128418–18.

51. Eylea Assessment report EMA (2012). https://www.ema.europa.eu/en/documents/assessment-report/eylea-epar-public-assessment-report_en.pdf.

52. Jakeman, L.B., Winer, J., Bennett, G.L., Altar, C.A., and Ferrara, N. (1992). Binding sites for vascular endothelial growth factor are localized on endothelial cells in adult rat tissues. J. Clin. Invest. *89*, 244–253.

53. Hwang, D.J., Kim, Y.W., Woo, S.J., and Park, K.H. (2012). Comparison of systemic adverse events associated with intravitreal anti-vegf injection: Ranibizumab versus bevacizumab. J. J. Kor. Med. Sci. *27*, 1580–1585.

54. Gaudana, R., Jwala, J., Boddu, S.H.S., and Mitra, A.K. (2009). Recent perspectives in ocular drug delivery. Pharm. Res. (N. Y.) *26*, 1197–1216.

55. Costa, R.A., Jorge, R., Calucci, D., Cardillo, J.A., Melo, L.A.S., and Scott, I.U. (2006). Intravitreal bevacizumab for choroidal neovascularization caused by AMD (IBeNA study): Results of a phase 1 dose-escalation study. Invest. Ophthalmol. Vis. Sci. *47*, 4569–4578.

56. Dalkara, D., Kolstad, K.D., Caporale, N., Visel, M., Klimczak, R.R., Schaffer, D.V., and Flannery, J.G. (2009). Inner limiting membrane barriers to aav-mediated retinal transduction from the vitreous. Mol. Ther. *17*, 2096–2102.

57. Boye, S.E., Alexander, J.J., Witherspoon, C.D., Boye, S.L., Peterson, J.J., Clark, M.E., Sandefer, K.J., Girkin, C.A., Hauswirth, W.W., and Gamlin, P.D. (2016). Highly efficient delivery of adeno-associated viral vectors to the primate retina. Hum. Gene Ther. *27*, 580–597.

58. Kotterman, M.A., Yin, L., Strazzeri, J.M., Flannery, J.G., Merigan, W.H., and Schaffer, D.V. (2015). Antibody neutralization poses a barrier to intravitreal adeno-associated viral vector gene delivery to non-human primates. Gene Ther. *22*, 116–126.

59. Ronzitti, G., Gross, D.A., and Mingozzi, F. (2020). Human Immune Responses to Adeno-Associated Virus (AAV) Vectors. Front. Immunol. *11*, 1–13.

60. Mingozzi, F., and High, K.A. (2007). Immune Responses to AAV in Clinical Trials. Curr. Gene Ther. *7*, 316–324.

61. Zaiss, A.K., and Muruve, D.A. (2005). Immune Responses to Adeno-Associated Virus Vectors. Curr. Gene Ther. *5*, 323–331.

62. Reichel, F.F., Peters, T., Wilhelm, B., Biel, M., Ueffing, M., Wissinger, B., Bartz-Schmidt, K.U., Klein, R., Michalakis, S., and Fischer, M.D.; RD-CURE Consortium (2018). Humoral immune response after intravitreal but not after subretinal aav8 in primates and patients. Invest. Ophthalmol. Vis. Sci. *59*, 1910–1915.

63. Rakoczy, E.P., Magno, A.L., Lai, C.M., Pierce, C.M., Degli-Esposti, M.A., Blumenkranz, M.S., and Constable, I.J. (2019). Three-Year Follow-Up of Phase 1 and 2a rAAV.sFLT-1 Subretinal Gene Therapy Trials for Exudative Age-Related Macular Degeneration. Am. J. Ophthalmol. *204*, 113–123.

64. Patel, P., and Sheth, V. (2021). New and Innovative Treatments for Neovascular Age-Related Macular Degeneration (nAMD). J. Clin. Med. *10*, 2436.

65. Bainbridge, J.W.B., Stephens, C., Parsley, K., Demaison, C., Halfyard, A., Thrasher, A.J., and Ali, R.R. (2001). In vivo gene transfer to the mouse eye using an HIV-based lentiviral vector; efficient long-term transduction of cornealendothelium and retinal pigment epithelium. Gene Ther. *8*, 1665–1668.

66. Binley, K., Widdowson, P., Loader, J., Kelleher, M., Iqball, S., Ferrige, G., de Belin, J., Carlucci, M., Angell-Manning, D., Hurst, F., et al. (2013). Transduction of photoreceptors with equine infectious anemia virus lentiviral vectors: Safety and biodistribution of stargen for stargardt disease. Invest. Ophthalmol. Vis. Sci. *54*, 4061–4071.

67. Zallocchi, M., Binley, K., Lad, Y., Ellis, S., Widdowson, P., Iqball, S., Scripps, V., Kelleher, M., Loader, J., Miskin, J., et al. (2014). EIAV-based retinal gene therapy in the shaker1 mouse model for usher syndrome type 1B: Development of UshStat. PLoS One *9*, e94272.

68. Binley, K., Widdowson, P.S., Kelleher, M., De Belin, J., Loader, J., Ferrige, G., Carlucci, M., Esapa, M., Chipchase, D., Angell-Manning, D., et al. (2012). Safety and biodistribution of an equine infectious anemia virus-based gene therapy, retinostat®, for age-related macular degeneration. Hum. Gene Ther. *23*, 980–991.

69. Miyoshi, H., Takahashi, M., Gage, F.H., and Verma, I.M. (1997). Stable and efficient gene transfer into the retina using an HIV-based lentiviral vector. Proc. Natl. Acad. Sci. U. S. A *94*, 10319–10323.

70. White, M., Whittaker, R., Gándara, C., and Stoll, E.A. (2017). A Guide to Approaching Regulatory Considerations for Lentiviral-Mediated Gene Therapies. Hum. Gene Ther. Methods *28*, 163–176.

71. Naso, M.F., Tomkowicz, B., Perry, W.L., and Strohl, W.R. (2017). Adeno-Associated Virus (AAV) as a Vector for Gene Therapy. BioDrugs *31*, 317–334.

72. Adverum Biotechnologies Presents Anatomical Improvements in Intraretinal and Subretinal Fluid After a Single IVT Injection of Ixo-vec (ADVM-022) in the OPTIC Study in Wet AMD (2022). https://investors.adverum.com/news/news-details/2022/Adverum-Biotechnologies-Presents-Anatomical-Improvements-in-Intraretinal-and-Subretinal-Fluid-After-a-Single-IVT-Injection-of-Ixo-vec-ADVM-022-in-the-OPTIC-Study-in-Wet-AMD/default.aspx.

73. Avery, R.L., Castellarin, A.A., Steinle, N.C., Dhoot, D.S., Pieramici, D.J., See, R., Couvillion, S., Nasir, M.A., Rabena, M.D., Maia, M., et al. (2017). Systemic pharmacokinetics and pharmacodynamics of intravitreal aflibercept, bevacizumab, and ranibizumab. Retina *37*, 1847–1858.

74. Long, D., Kanan, Y., Shen, J., Hackett, S.F., Liu, Y., Hafiz, Z., Khan, M., Lu, L., and Campochiaro, P.A. (2018). VEGF/VEGFR2 blockade does not cause retinal atrophy in AMD-relevant models. JCI insight *3*, 1–14.

75. Ueno, S., Pease, M.E., Wersinger, D.M.B., Masuda, T., Vinores, S.A., Licht, T., Zack, D.J., Quigley, H., Keshet, E., and Campochiaro, P.A. (2008). Prolonged blockade of VEGF family members does not cause identifiable damage to retinal neurons or vessels. J. Cell. Physiol. *217*, 13–22.

76. Miki, A., Miki, K., Ueno, S., Wersinger, D.M.B., Berlinicke, C., Shaw, G.C., Usui, S., Wang, Y., Zack, D.J., and Campochiaro, P.A. (2010). Prolonged blockade of VEGF receptors does not damage retinal photoreceptors or ganglion cells. J. Cell. Physiol. *224*, 262–272.

77. Gelfman, C.M., Grishanin, R., Bender, K.O., Nguyen, A., Greengard, J., Sharma, P., Nieves, J., Kiss, S., and Gasmi, M. (2021). Comprehensive Preclinical Assessment of ADVM-022, an Intravitreal Anti-VEGF Gene Therapy for the Treatment of Neovascular AMD and Diabetic Macular Edema. J. Ocul. Pharmacol. Therapeut. *37*, 181–190.

78. Maunder, H.E., Wright, J., Kolli, B.R., Vieira, C.R., Mkandawire, T.T., Tatoris, S., Kennedy, V., Iqball, S., Devarajan, G., Ellis, S., et al. (2017). Enhancing titres of therapeutic viral vectors using the transgene repression in vector production (TRiP) system. Nat. Commun. *8*, 14834.

79. Farley, D.C., Iqball, S., Smith, J.C., Miskin, J.E., Kingsman, S.M., and Mitrophanous, K.A. (2007). Factors that influence VSV-G pseudotyping and transduction efficiency of lentiviral vectors - *In vitro* and *in vivo* implications. J. Gene Med. *9*, 345–356.

80. Senova, S., Poupon, C., Dauguet, J., Stewart, H.J., Dugué, G.P., Jan, C., Hosomi, K., Ralph, G.S., Barnes, L., Drouot, X., et al. (2018). Optogenetic Tractography for anatomo-functional characterization of cortico-subcortical neural circuits in non-human primates. Sci. Rep. *8*, 3362–3412.

81. Kong, J., Kim, S.R., Binley, K., Pata, I., Doi, K., Mannik, J., Zernant-Rajang, J., Kan, O., Iqball, S., Naylor, S., et al. (2008). Correction of the disease phenotype in the mouse model of Stargardt disease by lentiviral gene therapy. Gene Ther. *15*, 1311–1320.

82. Wimmer, T., Lorenz, B., and Stieger, K. (2015). Functional characterization of AAV-expressed recombinant anti-VEGF single-chain variable fragments *in vitro*. J. Ocul. Pharmacol. Therapeut. *31*, 269–276.

83. Crouch, S.P., Kozlowski, R., Slater, K.J., and Fletcher, J. (1993). The use of ATP bioluminescence as a measure of cell proliferation and cytotoxicity. J. Immunol. Methods *160*, 81–88.

84. Nomoto, H., Shiraga, F., Kuno, N., Kimura, E., Fujii, S., Shinomiya, K., Nugent, A.K., Hirooka, K., and Baba, T. (2009). Pharmacokinetics of bevacizumab after topical, subconjunctival, and intravitreal administration in rabbits. Invest. Ophthalmol. Vis. Sci. *50*, 4807–4813.